Histone methylation readers MRG1/2 interact with PIF4 to promote thermomorphogenesis in Arabidopsis

Nana Zhou, Chengzhang Li, Wenhao Xie, Ning Liang, Jiachen Wang, Baihui Wang, Jiabing Wu, Wen-Hui Shen, Bing Liu, Aiwu Dong

▶ **To cite this version:**

Nana Zhou, Chengzhang Li, Wenhao Xie, Ning Liang, Jiachen Wang, et al.. Histone methylation readers MRG1/2 interact with PIF4 to promote thermomorphogenesis in Arabidopsis. Cell Reports, 2024, 43 (2), pp.113726. 10.1016/j.celrep.2024.113726 . hal-04456338

HAL Id: hal-04456338
https://hal.science/hal-04456338

Submitted on 13 Feb 2024

HAL is a multi-disciplinary open access archive for the deposit and dissemination of scientific research documents, whether they are published or not. The documents may come from teaching and research institutions in France or abroad, or from public or private research centers.

L'archive ouverte pluridisciplinaire **HAL**, est destinée au dépôt et à la diffusion de documents scientifiques de niveau recherche, publiés ou non, émanant des établissements d'enseignement et de recherche français ou étrangers, des laboratoires publics ou privés.

Cell Reports

Article

Histone methylation readers MRG1/2 interact with PIF4 to promote thermomorphogenesis in *Arabidopsis*

Graphical abstract

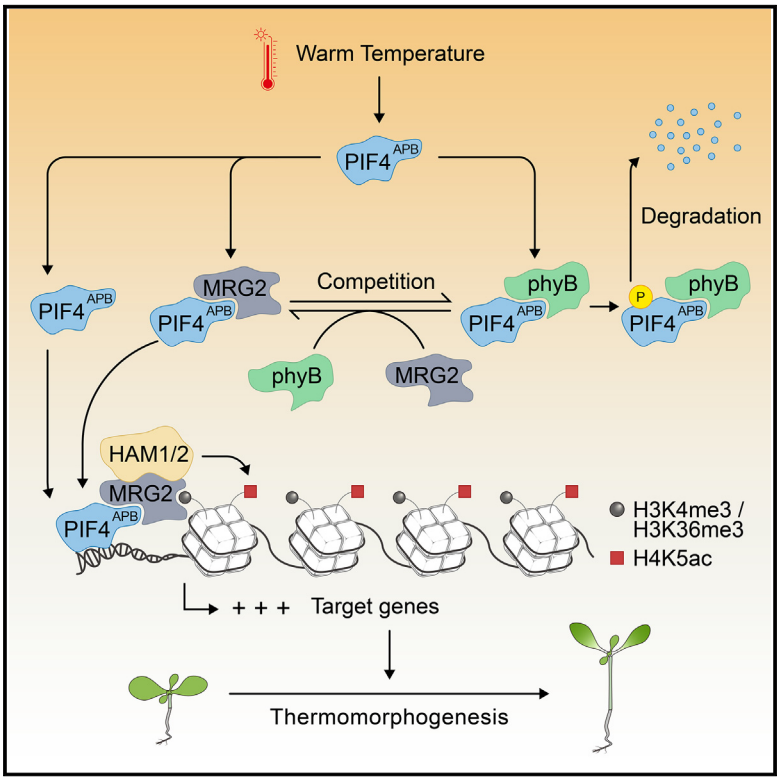

Highlights

- MRG1/2 promote hypocotyl elongation in response to warm ambient conditions
- MRG2 interacts with PIF4 to coactivate a set of thermoresponsive genes
- PIF4 recruits MRG2 to the target genes and enhances H4K5 acetylation upon warmth
- MRG2 binds to and stabilizes PIF4 protein by competing with phyB

Authors

Nana Zhou, Chengzhang Li, Wenhao Xie, ..., Wen-Hui Shen, Bing Liu, Aiwu Dong

Correspondence

bliu279@wisc.edu (B.L.), aiwudong@fudan.edu.cn (A.D.)

In brief

Warm temperature conditions induce thermomorphogenesis and influence plant growth and development. Zhou et al. show that histone methylation reader MRG2 competes with phyB to bind to and stabilize PIF4, which enhances H4K5 acetylation and activates the transcription of the thermoresponsive genes and promotes the warm response in *Arabidopsis*.

Zhou et al., 2024, Cell Reports *43*, 113726
February 27, 2024 © 2024 The Author(s).
https://doi.org/10.1016/j.celrep.2024.113726

CellPress

Cell Reports

CellPress
OPEN ACCESS

Article

Histone methylation readers MRG1/2 interact with PIF4 to promote thermomorphogenesis in *Arabidopsis*

Nana Zhou,[1,4] Chengzhang Li,[1,4] Wenhao Xie,[1] Ning Liang,[1] Jiachen Wang,[1] Baihui Wang,[1] Jiabing Wu,[1] Wen-Hui Shen,[2] Bing Liu,[1,3,*] and Aiwu Dong[1,5,*]

[1]State Key Laboratory of Genetic Engineering, Collaborative Innovation Center for Genetics and Development, Department of Biochemistry and Biophysics, Institute of Plant Biology, School of Life Sciences, Fudan University, Shanghai 200438, P.R. China
[2]Institut de Biologie Moléculaire des Plantes, CNRS, Université de Strasbourg, 12 rue du Général Zimmer, 67084 Strasbourg Cédex, France
[3]Department of Energy, Great Lakes Bioenergy Research Center, University of Wisconsin–Madison, Madison, WI 53706, USA
[4]These authors contributed equally
[5]Lead contact
*Correspondence: bliu279@wisc.edu (B.L.), aiwudong@fudan.edu.cn (A.D.)
https://doi.org/10.1016/j.celrep.2024.113726

SUMMARY

Warm ambient conditions induce thermomorphogenesis and affect plant growth and development. However, the chromatin regulatory mechanisms involved in thermomorphogenesis remain largely obscure. In this study, we show that the histone methylation readers MORF-related gene 1 and 2 (MRG1/2) are required to promote hypocotyl elongation in response to warm ambient conditions. A transcriptome sequencing analysis indicates that *MRG1/2* and *phytochrome interacting factor 4* (*PIF4*) coactivate a number of thermoresponsive genes, including *YUCCA8*, which encodes a rate-limiting enzyme in the auxin biosynthesis pathway. Additionally, MRG2 physically interacts with PIF4 to bind to thermoresponsive genes and enhances the H4K5 acetylation of the chromatin of target genes in a PIF4-dependent manner. Furthermore, MRG2 competes with phyB for binding to PIF4 and stabilizes PIF4 *in planta*. Our study indicates that MRG1/2 activate thermoresponsive genes by inducing histone acetylation and stabilizing PIF4 in *Arabidopsis*.

INTRODUCTION

Temperature is one of the most important environmental factors for plant growth and development, with ambient temperatures substantially affecting plant distribution and seasonal behaviors.[1–3] As sessile species, plants adapt to warm ambient conditions via a series of morphological changes (i.e., thermomorphogenesis).[4,5] In *Arabidopsis thaliana* (Arabidopsis), typical thermomorphogenic changes include hypocotyl and petiole elongation, leaf hyponasty, and early flowering, which enable plants to form a separate rosette structure away from warm soil, thereby enhancing growth and development.[6,7]

The key regulator of thermomorphogenesis is the basic helix-loop-helix (bHLH) transcription factor PHYTOCHROME INTERACTING FACTOR 4 (PIF4), which was first identified as a protein that binds to the photoreceptor phytochrome B (phyB).[8,9] Previous studies determined that *PIF4* expression is rapidly induced following an increase in the ambient temperature and that the *pif4* mutant lacks the hypocotyl elongation response under warm conditions.[10,11] In addition, PIF4 promotes auxin biosynthesis/signaling by binding to and activating a set of genes, including *YUCCA8* (*YUC8*), *SMALL AUXIN UP RNA* (*SAUR*), and *INDOLE-3-ACETIC ACID INDUCIBLE 19*, to induce thermomorphogenic changes (e.g., hypocotyl elongation).[10,12–16] As a crucial regulator of PIF4 stability, phyB is involved in the posttranscriptional regulation of *PIF4*.[5] The evening complex components, including EARLY FLOWERING 3 (ELF3), ELF4, and LUX ARRHYTHMO (LUX), regulate the proper transcription of *PIF4*.[17,18] LONG HYPOCOTYL 5 (HY5), a bZIP transcription factor, directly binds to the promoter region of *PIF4* to repress *PIF4* transcription.[19,20] ELF3 and the evening-expressed circadian clock protein TIMING OF CAB EXPRESSION1 directly interact with PIF4 and prevent PIF4 from activating its target genes.[21,22] B-BOX PROTEIN 11 interacts with PIF4 and inhibits the accumulation of PIF4 protein.[23] BLADE-ON-PETIOLE promotes the red light-induced reduction of PIF4 protein.[24] Aspartic acid-glutamic acid-leucine-leucine-alanine (DELLA) proteins inhibit the transcriptional activity of PIF4 by preventing PIF4 from binding to the target genes.[25] In addition, the stability of PIF4 is regulated by DE-ETIOLATED1 (DET1), BRASSINOSTEROIDINSENSITIVE 2 (BIN2), CONSTITUTIVE PHOTOMORPHOGENIC1, SUPPRESSOR OF PHYA-105 (SPA), HEMERA (HMR), and REGULATOR OF CHLOROPLAST BIOGENESIS (RCB).[19,26–30] The transcription

This is an open access article under the CC BY-NC-ND license (http://creativecommons.org/licenses/by-nc-nd/4.0/).

factor TEOSINTE BRANCHED 1/CYCLOIDEA/PCF 5 and MYB30 promote the activity of PIF4 at both transcriptional and posttranslational levels.[31,32] Notably, the photoreceptor phyB also functions as a thermosensor, for upon warm treatment, Pfr phyB (active form) spontaneously reverts to Pr phyB (inactive form).[33–36] After binding to Pfr phyB, PIF4 is phosphorylated, ubiquitinated, and finally degraded by a proteasome.[37]

Recent research revealed that some chromatin regulatory mechanisms modulate thermomorphogenesis. For example, ACTIN-RELATED PROTEIN 6 (ARP6), a component of the SWR1 chromatin remodeling complex, incorporates H2A.Z into chromatin; Arabidopsis plants lacking ARP6 exhibit constitutive elevated temperature-induced phenotypes even at normal temperatures.[38] Moreover, Arabidopsis plants lacking the chromatin remodeling factor INOSITOL REQUIRING 80 (INO80) are unresponsive to elevated temperatures; INO80 interacts with PIF4 and promotes thermomorphogenesis by activating the transcription of PIF4 target genes.[39] In addition to chromatin remodeling, covalent modifications of histones are involved in Arabidopsis thermomorphogenesis. The histone deacetylases HISTONE DEACETYLASE 9 (HDA9), HDA15, and HDA19 are involved in thermomorphogenesis regulation.[40–42] The H3K27 demethylase RELATIVE OF ELF6 functions cooperatively with PIF4 to synergistically promote thermomorphogenesis by activating the transcription of thermoresponsive genes under warm ambient conditions.[43] The chromatin remodeling factor PICKLE is a positive regulator in thermomorphogenesis by affecting H3K27me3 modification at thermoresponsive genes.[44] Finally, the histone H3K4 demethylases Jumonji C 14 (JMJ14), JMJ15, and JMJ18 function redundantly in response to warm temperatures by repressing the transcription of a subset of temperature-responsive genes.[45]

The histone methylation readers MORF-related gene 1 and 2 (MRG1/2) were first identified as H3K4me2/me3 and H3K36me2/me3 readers that promote flowering by interacting with CONSTANS to modulate *FLOWERING LOCUS T* expression in Arabidopsis.[46] In addition, MRG1/2 interact with the H4-specific acetyltransferases HISTONE ACETYLTRANSFERASE OF THE MYST FAMILY 1 and 2 (HAM1/2), the histone chaperones NAP1-RELATED PROTEIN 1 and 2, and the histone deacetylase HISTONE DEACETYLASE 2C (HD2C) to regulate the expression of flowering genes.[47–49] In addition, MRG1/2 promote shade-induced hypocotyl elongation by interacting with the transcription factor PIF7.[50]

Here, we report that MRG1/2 promote thermomorphogenesis by activating PIF4 target genes. We observed that the *mrg1 mrg2* double mutant failed to respond to elevated ambient temperatures, similar to the *pif4* mutant. Our transcriptome sequencing (RNA-seq) analysis revealed that the expression levels of several thermoresponsive genes (e.g., *YUC8*, *SAUR19*, *PAR1*) were downregulated in the *mrg1 mrg2*, *pif4*, and *mrg1 mrg2 pif4* mutants under warm conditions. Our findings indicate that the histone reader proteins MRG1/2 form a complex with PIF4 to activate thermoresponsive genes, while also stabilizing PIF4 at the protein level, which is a novel mechanism for the chromatin regulation of thermomorphogenesis in plants.

RESULTS

MRG1/2 positively regulate plant responses to warm ambient conditions

The analysis of RNA-seq data[47,49] detected the misregulation of multiple hormone-related genes in the *mrg1 mrg2* double mutant, including the auxin synthesis genes *SAUR19–SAUR25* and *SAUR57*, the auxin- and brassinosteroid-responsive gene *PAR1*, and *PRE1*. Because phytohormones are essential for thermomorphogenesis,[51,52] our observations prompted us to investigate whether MRG1/2 contribute to thermomorphogenesis. During the incubation at 22°C (i.e., normal conditions), the *mrg1 mrg2* mutant and the wild-type (WT) control had similar hypocotyl lengths, whereas at 28°C (i.e., warm conditions) the WT hypocotyl elongated significantly more than the *mrg1 mrg2* hypocotyl (Figures 1A and S1A), although the *mrg1* and *mrg2* single mutants behaved similarly to the WT plants at 28°C (Figure 1A). The expression of *MRG2-Myc* driven by the *MRG2* promoter in the *mrg1 mrg2* double mutant resulted in plants that responded normally to warm conditions (i.e., similarly to the WT plants) (Figure 1A), suggesting that *MRG1/2* redundantly promote hypocotyl elongation under warm conditions. We also tested the petiole elongation and leaf hyponasty of the *mrg1 mrg2* mutant in response to warm temperatures. Compared to the WT plants, the *mrg1 mrg2* mutant exhibited a weaker response to warm treatment both in petiole length and leaf hyponasty (Figures 1C and S2). Taken together, *MRG1/2* are necessary for the proper response to warm ambient temperatures in Arabidopsis.

MRG1/2 and *PIF4* coactivate a subset of thermoresponsive genes

In accordance with the fact that PIF4 functions as a central regulator of thermomorphogenesis, the elongation of hypocotyl and petiole induced by warm conditions (28°C) was repressed in the *pif4* mutant (Figures 1B and 1C). To examine the genetic relationship between *MRG1/2* and *PIF4*, we crossed *mrg1 mrg2* with *pif4* to generate the *mrg1 mrg2 pif4* triple mutant. After an exposure to warm ambient conditions, the defective elongation of hypocotyl and petiole in the *mrg1 mrg2 pif4* triple mutant was similar to that in the *pif4* mutant, but was stronger than that in the *mrg1 mrg2* double mutant (Figures 1B and 1C), implying that *PIF4* acts epistatically to *MRG1/2* to promote hypocotyl and petiole elongation. Consistent with the epistasis relationship between *MRG1/2* and *PIF4*, the leaf hyponasty in *mrg1 mrg2 pif4* triple mutant exhibited similarly to that observed in the *pif4* mutant (Figure S2).

To explore how MRG1/2 affect thermomorphogenesis, we conducted an RNA-seq analysis of WT, *mrg1 mrg2*, *pif4*, and *mrg1 mrg2 pif4* plants incubated at 22°C and 28°C. We completed a pairwise scatterplot analysis to investigate the regulatory effects of MRG1/2 and PIF4 on transcription under normal (22°C) and warm (28°C) conditions. This analysis revealed that the misregulated genes in the *pif4* and *mrg1 mrg2* mutants were highly correlated (Figure 2A; Table S2). According to the RNA-seq data for the WT plants, the expression levels of 932 and 1,361 genes were respectively up- and downregulated at 28°C by more than 1.5-fold ($p < 0.05$) (Figure 2B; Table S2).

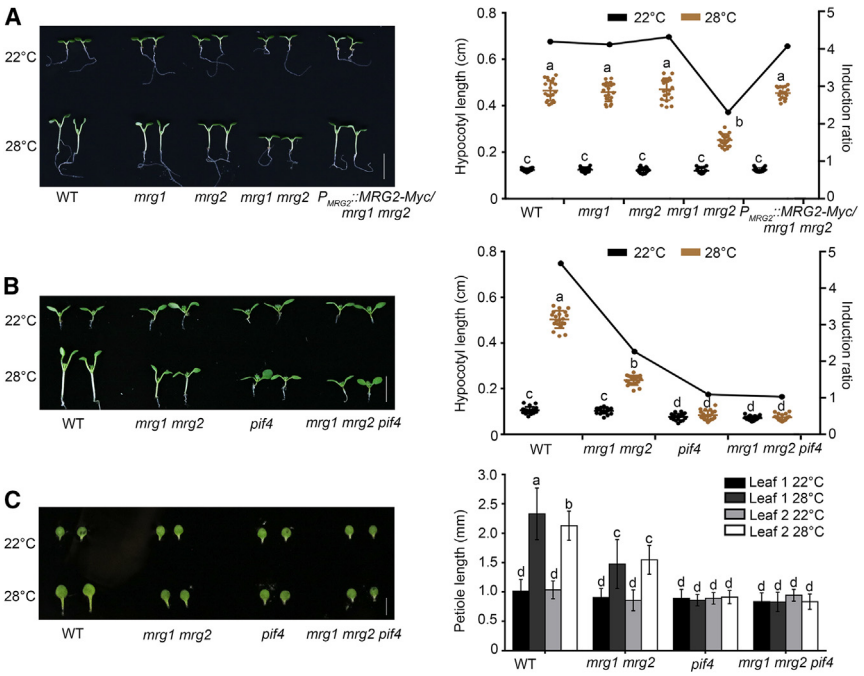

Figure 1. *MRG1/2* are required for elevated temperature-induced hypocotyl elongation and petiole elongation

(A) Phenotypes of WT, *mrg1*, *mrg2*, *mrg1 mrg2*, and P_{MRG2}*::MRG2-Myc/mrg1 mrg2* plants at 22°C (normal conditions) or 28°C (warm conditions). Scale bar, 0.5 cm.

(B) Phenotypes of WT, *mrg1 mrg2*, *pif4*, and *mrg1 mrg2 pif4* plants at 22°C (normal conditions) or 28°C (warm conditions). Scale bar, 0.5 cm.

(C) The petiole length of WT, *mrg1 mrg2*, *pif4*, and *mrg1 mrg2 pif4* plants at 22°C (normal conditions) or 28°C (warm conditions). Scale bar, 0.5 cm.

For (A) and (B), The left y axis presents the hypocotyl length, whereas the right y axis presents the ratio of the hypocotyl length at 28°C to that at 22°C. The hypocotyl length and the petiole length for the indicated genotypes were calculated using at least 20 plants (one-way ANOVA, followed by Fisher's least significant difference [LSD] test; $p < 0.05$).

The numbers of misregulated genes in the *mrg1 mrg2*, *pif4*, and *mrg1 mrg2 pif4* mutants are presented in Figure 2B. We selected the differentially expressed genes (DEGs) in WT at 28°C, and further analyzed their fold changes (28°C/22°C) in the *mrg1 mrg2*, *pif4*, and *mrg1 mrg2 pif4* plants. The DEGs in WT were divided into four clusters (Figure 2C). The genes in clusters 1 and 4 were respectively down- and upregulated in the WT plants and the three mutants under warm conditions. The cluster 2 genes were significantly downregulated in the WT control, but not in the mutants, whereas the cluster 3 genes were substantially upregulated in the WT control, but not in the mutants under warm conditions.

To investigate the distribution of PIF4 along chromatin in response to warm temperatures, we performed chromatin immunoprecipitation sequencing (ChIP-seq) analysis by using P_{PIF4}*::PIF4-HA/pif4* plants at 22°C and 28°C. A total of 5,416 peaks corresponding to 4,890 genes were identified as the PIF4-occupied peaks (Figures 3A and 3B; Table S3). PIF4 mainly enriched around the regions close to the transcription start site (TSS) (Figures 3A and S3A), consistent with its role as a transcription factor. A significant overlap was observed between PIF4 targets and the genes in clusters 2 and 3, where genes were improperly induced or repressed by warm treatment in the mutants (Figures 2C, 3B, S3B, and S3C; Table S4). Gene Ontology analysis using the overlapped genes with cluster 2, cluster 3, or clusters 2/3 showed that these genes are involved in many biological processes, including response to hormones (Figures 3C, S3D, and S3E). Considering that hormones (e.g., auxin, gibberellins, brassinosteroid) have been reported to function in the control of hypocotyl elongation,[5] we focused on the genes in the catalog of response to hormone for further analysis (Figure 3D). A set of genes in this catalog were previously reported to be induced by warm ambient conditions, such as auxin synthesis genes (*YUC8* and *SAUR19*) and the auxin- and brassinosteroid-responsive gene *PAR1*, which are the central thermoinduced genes (Figure 3D). Our ChIP-seq data clearly showed that PIF4 significantly enriched at the 5′ upstream of *YUC8*, *SAUR19*, and *PAR1* genes at 28°C compared to at 22°C (Figure 3E). Consistently, the transcript levels of *YUC8*, *SAUR19*, and *PAR1* in WT at 28°C are obviously higher than those at 22°C and in the mutant plants at 22°C/28°C (Figure 3E). Quantitive reverse transcription PCR (qRT-PCR) analysis further confirmed that the transcription of *YUC8*, *SAUR19*, and *PAR1* decreased in the *mrg1 mrg2*, *pif4*, and *mrg1 mrg2 pif4* mutants compared to the WT control at 28°C (Figure S3F). Together, our results indicate that MRG1/2 and PIF4 co-regulate a set of thermoresponsive genes to promote thermomorphogenesis in Arabidopsis.

MRG1/2 physically interact with PIF4

The genetic analysis confirmed that *MRG1/2* and *PIF4* affect the same pathway during thermomorphogenesis (Figures 1B, 1C, and S2). The qRT-PCR results showed that the deletion of *MRG1/2* did not affect *PIF4* transcription and the deletion of *PIF4* had no effect on *MRG1/2* transcription at both 22°C and 28°C (Figures S1B and S1C), which compelled us to assess whether MRG1/2 interact with PIF4. The yeast two-hybrid (Figure 4A), glutathione S-transferase (GST) pulldown (Figure 4B), and biomolecular fluorescence complementation (BiFC) (Figure 4C) assays demonstrated the physical interaction between MRG2 and PIF4 *in vitro* and *in vivo*. Specifically, yellow fluorescent protein (YFP) signals were restricted to the nucleus, which is where MRG2 and PIF4 were localized (Figure 4C). We also generated transgenic plants overexpressing *Flag-MRG2* and *PIF4-HA* for a coimmunoprecipitation (coIP) assay. The hemagglutinin (HA)-tagged PIF4 protein precipitated with the Flag-tagged MRG2 (Figure 4D). Moreover, MRG1, which is homologous to MRG2, also interacted with PIF4 in the GST pulldown

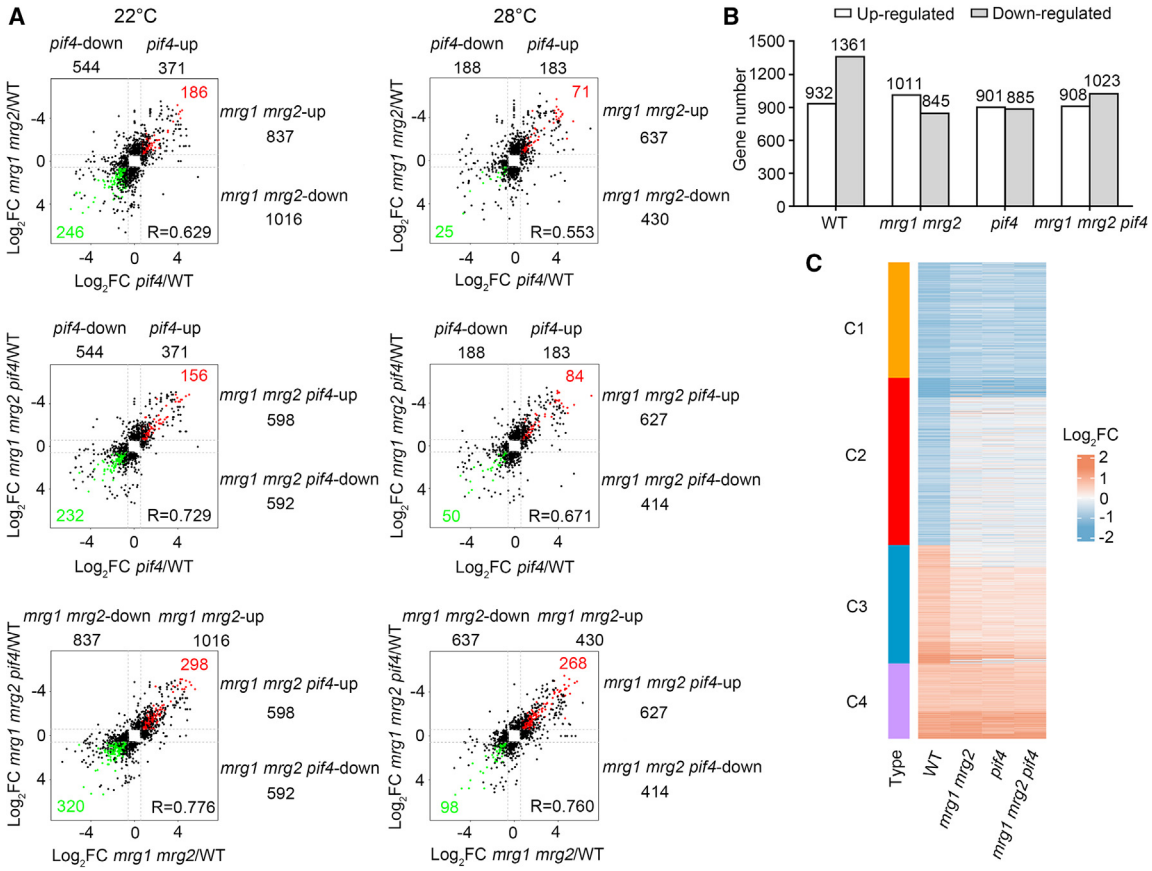

Figure 2. *MRG1/2* and *PIF4* co-regulate a set of genes

(A) Pairwise scatterplot analysis showing the highly correlated DEGs ($p < 0.05$ and fold change >1.5) in the *mrg1 mrg2*, *pif4*, and *mrg1 mrg2 pif4* plants (compared with the WT controls) at 22°C (left) and 28°C (right). The numbers of up- and downregulated genes ($p < 0.05$ and fold change >1.5) in the *mrg1 mrg2*, *pif4*, and *mrg1 mrg2 pif4* mutants are presented (compared with the WT controls). Red and green dots/numbers represent the co-up- and co-downregulated genes, respectively.

(B) Numbers of up- and downregulated genes ($p < 0.05$ and fold change >1.5) in the WT, *mrg1 mrg2*, *pif4*, and *mrg1 mrg2 pif4* plants at 28°C are presented (compared with the plants at 22°C).

(C) Heatmap presenting the $\log_2$FC (fold change) of DEGs in WT at 28°C compared to at 22°C, and the $\log_2$FC (28°C/22°C) of these genes in the *mrg1 mrg2*, *pif4*, and *mrg1 mrg2 pif4* mutant plants.

assay (Figure S4). These results reflected the physical interaction between the histone methylation readers MRG1/2 and the transcription factor PIF4 in Arabidopsis.

The PIF4 protein has an N-terminal active phytochrome binding (APB) domain that is necessary for phyB binding as well as a C-terminal bHLH binding domain.[53] To determine which PIF4 domain is required for the interaction with MRG2, we generated four constructs encoding the following truncated PIF4 proteins: PIF4-N1 containing the APB domain (amino acids 1–50), PIF4-N2 (amino acids 51–253), PIF4-C1 (amino acids 254–430), and PIF4-C2 containing the bHLH binding domain (amino acids 51–430) (Figure 4E). The His-MRG2 fusion protein was precipitated in the pulldown assay by GST-PIF4-N1, but not by GST-PIF4-N2, GST-PIF4-C1, and GST-PIF4-C2 (Figure 4F). The BiFC assay provided additional evidence that only PIF4-N1 is necessary for the binding to MRG2 (Figure 4G), indicating that the PIF4 N-terminal (amino acids 1–50) containing the APB domain is sufficient for the MRG2–PIF4 interaction.

MRG2 binds to thermoresponsive gene loci in a PIF4-dependent manner

Consistent with the previous studies[16,54] and our ChIP-seq data (Figure 3E), our ChIP-quantitative PCR (ChIP-qPCR) results further confirmed that PIF4 binds to the *YUC8*, *SAUR19*, and *PAR1* promoter regions under warm conditions (Figures 5A and 5B). We subsequently investigated whether MRG2 binds to these genes by using the P_{MRG2}*::MRG2-Myc/mrg1 mrg2* and P_{MRG2}*::MRG2-Myc/mrg1 mrg2 pif4* transgenic plants, which expressed comparable MRG2-Myc protein in the *mrg1 mrg2* and *mrg1 mrg2 pif4* genetic backgrounds, respectively (Figure S5A). MRG2-Myc significantly enriched at the chromatin regions of *YUC8*, *SAUR19*, and *PAR1* genes at 28°C in the *mrg1 mrg2* background (Figures 5C, S5B, and S5C), but not in the *mrg1 mrg2 pif4* background (Figure 5D), indicating that the binding of MRG2 to the central thermoresponsive genes *YUC8*, *SAUR19*, and *PAR1* requires PIF4.

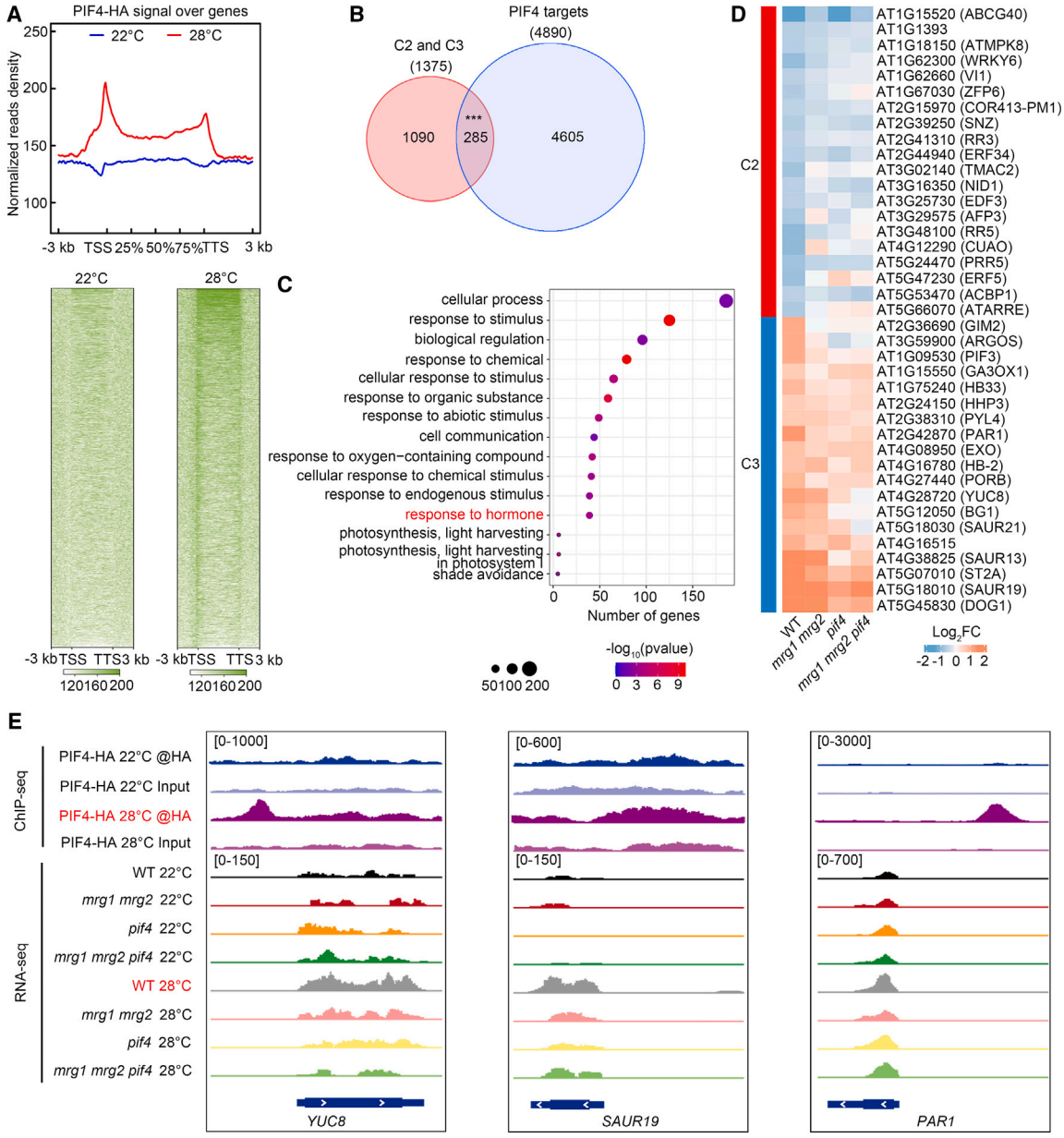

Figure 3. MRG1/2–PIF4 promote thermomorphogenesis by co-regulating a set of thermo-responsive genes

(A) ChIP-seq analysis showing the distribution of PIF4-HA along the genome in P_{PIF4}::*PIF4-HA*/*pif4* plants at 22°C and at 28°C. Heatmap (bottom) showing the gene-by-gene enrichment of PIF4-HA at PIF4 target genes (from 3 kb upstream TSS to 3 kb downstream transcription termination site [TTS]).

(B) Venn diagram showing comparison of genes in clusters 2/3 and the targets of PIF4. The significance level of the intersection was examined by single-end Fisher's exact test: ***$p < 0.001$.

(C) Functional enrichment analysis of the overlapped genes in (B). The size of each point represents the number of genes, and p values are indicated with various colors.

(D) Heatmap presenting the log_2FC (28°C/22°C) of genes involved in response to hormones in (C) in the WT, *mrg1 mrg2*, *pif4*, and *mrg1 mrg2 pif4* plants.

(E) Integrative Genomics Viewer shots showing the PIF4-HA ChIP-seq data at *YUC8*, *SAUR19*, and *PAR1* genes at 22°C and 28°C, and the RNA-seq data for these three genes in the WT, *mrg1 mrg2*, *pif4*, and *mrg1 mrg2 pif4* plants at 22°C and 28°C.

MRG1/2 and PIF4 induce the transcription of thermoresponsive genes via histone acetylations

As important chromatin regulatory factors, MRG1/2 are reader proteins that specifically recognize methylated H3K4 and H3K36.[46] In addition, MRG1/2 physically interact with the histone H3 deacetylase HD2C[49] and the histone H4 acetyltransferases HAM1 and HAM2.[48] Accordingly, we examined whether MRG-PIF4 induces the expression of thermoresponsive genes by regulating gene activation-related histone modifications. We first tested by western blot whether the global levels of

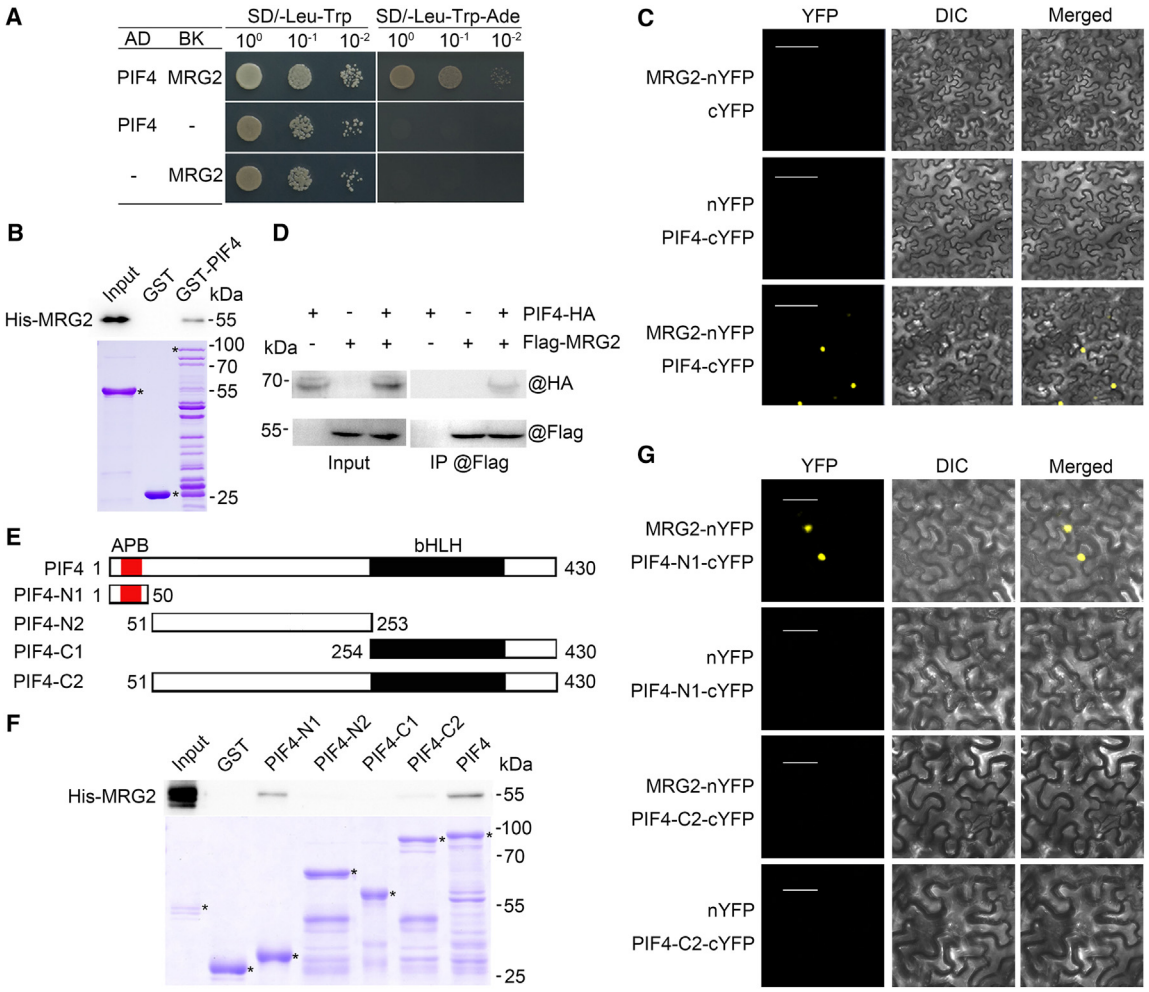

Figure 4. MRG2 interacts with PIF4 *in vitro* and *in vivo*

(A) Yeast two- hybrid assay showing the interaction between MRG2 and PIF4 in yeast cells.

(B) GST pulldown assay indicating that MRG2 interacted with PIF4 *in vitro*. His-MRG2 was pulled down by GST-PIF4, but not by GST. His-MRG2, GST, and GST-PIF4 proteins are marked by asterisks in the gel stained with Coomassie brilliant blue.

(C) BiFC assay showing the interaction between MRG2 and PIF4 in *N. benthamiana* leaf epidermal cells. Scale bar, 100 μm.

(D) The interaction between MRG2 and PIF4 was detected in a coIP assay. Proteins were extracted from 6-day-old plants overexpressing *Flag-MRG2*, *PIF4-HA*, or *Flag-MRG2/PIF4-HA*. Flag-MRG2 and PIF4-HA were detected in a western blot using anti-Flag and anti-HA antibodies, respectively.

(E) Schematic representation of the full-length and truncated PIF4 proteins.

(F) GST pulldown assay showing that His-MRG2 was pulled down by GST-PIF4-N1 and GST-PIF4. His-MRG2, GST-PIF4-N1, GST-PIF4-N2, GST-PIF4-C1, GST-PIF4-C2, and GST-PIF4 (full length) are marked by asterisks in the gel stained with Coomassie brilliant blue.

(G) BiFC assay showing that MRG2 interacted with the N terminus of PIF4 in tobacco leaf cells. Scale bar, 50 μm.

active histone modifications, including H3K4me3, H3K36me3, H3K9ac, H4K5ac, and H3K36ac, were affected by warm treatment. As shown in Figure S6A, warm temperatures did not induce obviously global changes of these histone modifications. Next, we performed ChIP-qPCR assay to test the levels of these modifications at *YUC8*, *SAUR19*, and *PAR1* loci. There were no obvious differences in the H3K4me3 and H3K36me3 levels at the *YUC8* locus between the treatment at 28°C and the treatment at 22°C (Figures S6B–S6D). In contrast, the H3K9ac and H4K5ac levels, but not the H3K36ac level, at the *YUC8* locus were significantly higher at 28°C than at 22°C, especially within the gene body region (Figures 6A–6D), indicating that H3K9ac and H4K5ac may be important for the activation of MRG-PIF4 targets during thermomorphogenesis.

A ChIP-qPCR analysis was performed to measure the histone acetylation levels at the PIF4 target gene loci in the WT, *mrg1 mrg2*, *pif4*, and *mrg1 mrg2 pif4* plants grown at 22°C and 28°C. The treatment at 28°C significantly increased the H3K9ac and H4K5ac levels at *YUC8* fragments 3 and 4 in the WT control and in the *mrg1 mrg2* mutant, but not in the *pif4* or *mrg1 mrg2 pif4* mutants (Figures 6E and 6F). However, the increase in H4K5ac level at *YUC8* at 28°C in the *mrg1 mrg2* mutant was significantly lower than that in WT (Figure 6F). Similarly, the H4K5ac levels of *SAUR19* and *PAR1* decreased significantly in

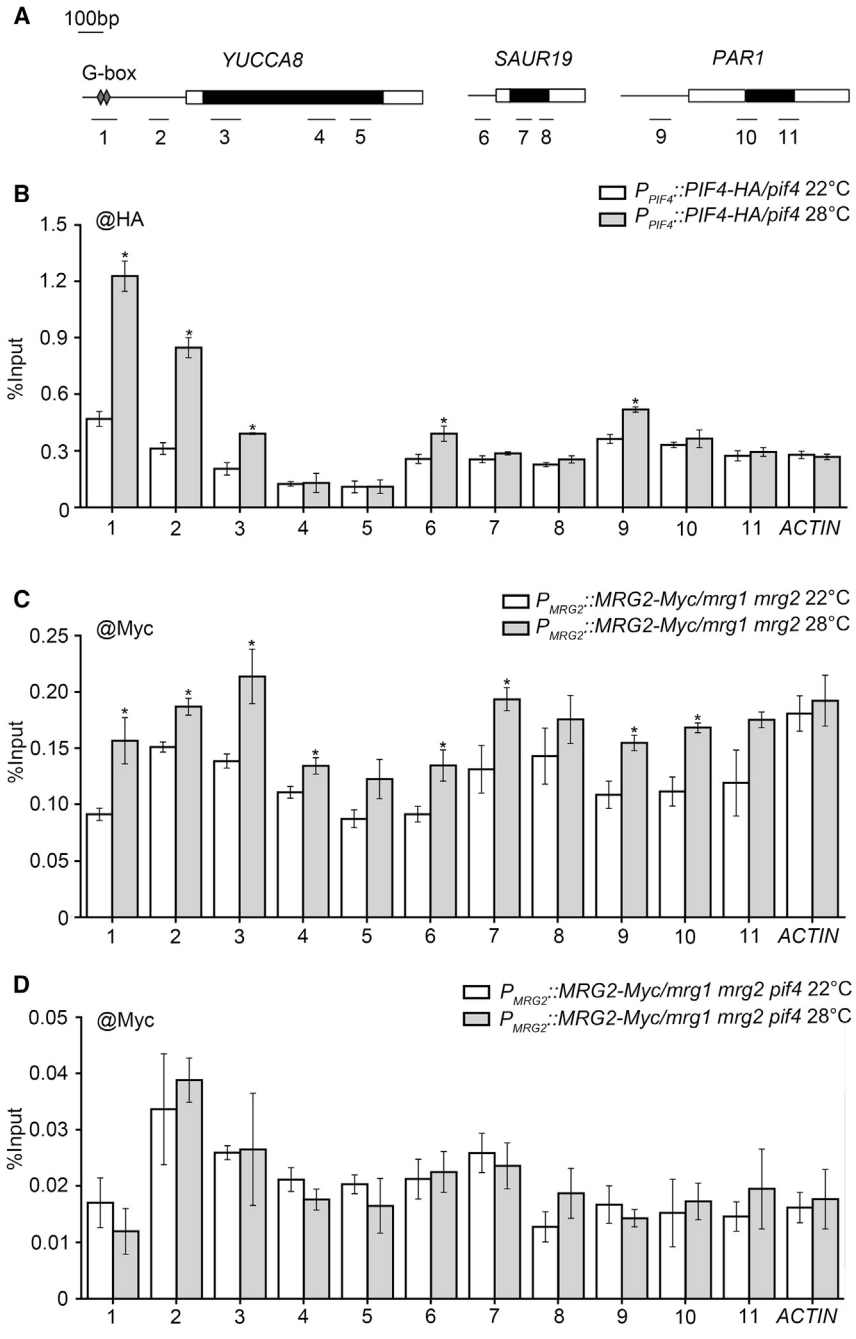

Figure 5. MRG2 and PIF4 bind to the chromatin regions of *YUC8*, *SAUR19*, and *PAR1* genes

(A) Schematic representation of *YUC8*, *SAUR19*, and *PAR1* genes and the fragments examined by ChIP-qPCR.

(B–D) ChIP analysis for PIF4/MRG2 enrichment at *YUC8*, *SAUR19*, and *PAR1* genes by using the antibody against HA in the transgenic P_{PIF4}::*PIF4-HA/pif4* plants (B) and the antibody against Myc in the P_{MRG2}::*MRG2-Myc/mrg1 mrg2* plants (C) and in the P_{MRG2}:: *MRG2-Myc/mrg1 mrg2 pif4* plants (D) at 22°C and 28°C. Values are presented as the mean ± SD of three individual biological replicates. *ACTIN2* acts as an internal control. Asterisks indicate significant differences between 22°C and 28°C (Student's t test; $p < 0.05$).

the examined mutants (Figures S6E–S6G). ChIP-seq analysis showed that the warm treatment at 28°C failed to result in a global change in the distributions of H3K9ac and H4K5ac along the genome in the WT and *pif4* mutant plants (Figure S7A). Consistent with our ChIP-qPCR results, the ChIP-seq analysis showed that 28°C treatment failed to induce the increase in H3K9ac at *YUC8* and *PAR1* genes in the *pif4* mutant compared to WT (Figure S7; Table S5). Considering *YUC8*, *SAUR19*, and *PAR1* lowly marked by H4K5ac and the different experiment assays for ChIP-qPCR and ChIP-seq, the H4K5ac changes at these genes in the *pif4* mutant and WT plants at 28°C were not detected in the ChIP-seq analysis (Figure S7). Taken together, our results implied that MRG1/2 and PIF4 are required for the induction of histone acetylation at thermoresponsive genes following an exposure to warm conditions.

MRG2 stabilizes PIF4 by competing with phyB

The MRG2 protein interacted with the PIF4 N terminus containing the APB domain, which is also responsible for the binding to phyB, prompting us to investigate whether the interaction between MRG2 and PIF4 affects the interaction between PIF4 and phyB. An *in vitro* competitive binding assay was performed, which showed that phyB strongly interacted with His-PIF4, but increasing amounts of MRG2 significantly weakened the interaction between phyB and PIF4 (Figures 7A and S8A). In addition, the GST pulldown assay involving *35S::Flag-MRG2*/Col-0 transgenic plants overexpressing *Flag-MRG2* in the WT genetic background demonstrated that the addition of Flag-MRG2 proteins extracted from Arabidopsis also inhibited the phyB–PIF4 interaction (Figure 7B). These findings suggest that MRG2 competes with phyB for the binding to PIF4.

To elucidate the competition between MRG2 and phyB *in vivo*, we performed a split luciferase assay in *Nicotiana benthamiana* leaves. Consistent with our *in vitro* results, the increase in MRG2 significantly blocked the interaction between PIF4 and phyB *in planta* (Figures 7C and S8B). In addition, we found that the increase in WT phyB also inhibited the interaction between MRG2 and PIF4 (Figures S8C and S8D). Furthermore, a point mutation in the N-terminal of phyB ($phyB^{G111D}$), which disturbs the interaction between phyB and

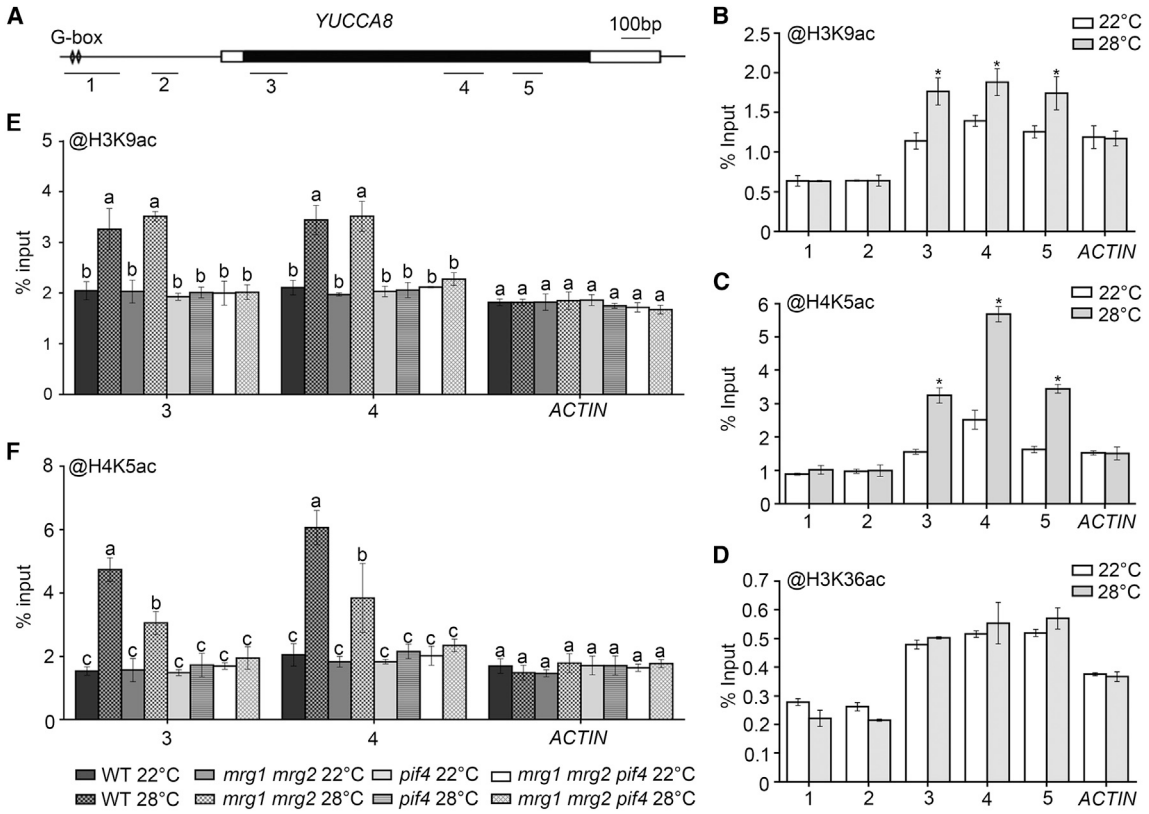

Figure 6. MRG1/2 and PIF4 promote the histone acetylation of thermoresponsive genes

(A) Schematic representation of the *YUC8* structures and fragments examined by ChIP-qPCR.

(B–D) ChIP analysis of *YUC8* using antibodies against H3K9ac (B), H4K5ac (C), and H3K36ac (D) for the WT plants incubated at 22°C and 28°C.

(E and F) ChIP analysis of *YUC8* using antibodies against H3K9ac (E) and H4K5ac (F) for the WT, *mrg1 mrg2*, *pif4*, and *mrg1 mrg2 pif4* plants incubated at 22°C and 28°C.

(B–F) Values are presented as the mean ± SD of three individual biological replicates, with *ACTIN2* serving as the control.

(B–D) Asterisks indicate significant differences between 22°C and 28°C in WT (Student's t test; $p < 0.05$).

(E and F) Significant differences between means are calculated by one-way ANOVA, followed by Fisher's LSD test ($p < 0.05$).

PIF4,[55] failed to block the MRG2-PIF4 interaction (Figures S8E and S8F).

To further investigate the role of MRG2 in competition with phyB to interact with PIF4 *in vivo*, we detected the PIF4 protein accumulation in the WT and *mrg1 mrg2* plants. Consistent with the results of earlier investigations,[10,11] under warm conditions, PIF4 accumulated in the WT control (Figures 7D and S9A), but the MRG2 abundance in the P_{MRG2}*::MRG2-Myc/mrg1 mrg2* plants was unchanged during the long-term exposure to warm conditions (Figure S9B). In contrast, the PIF4 content was significantly lower in the *mrg1 mrg2* mutant than in the WT control, even though PIF4 production was still induced in the *mrg1 mrg2* mutant during the prolonged exposure to warm conditions (Figure 7D). More important, the rapid degradation of PIF4 in *mrg1 mrg2* could be inhibited by MG132 treatment (Figure 7E). In addition, we observed a significant increase in PIF4 ubiquitination in the *mrg1 mrg2* mutant under warm conditions compared to WT (Figure S9C), indicating that MRG2 inhibited the degradation of PIF4 via the ubiquitin/proteasome pathway under warm conditions. Thus, the absence of MRG1/2 enhanced the interaction between PIF4 and phyB, leading to an increased degradation of PIF4. In addition, we examined the levels of the PIF4 protein in WT and the *35S::Flag-MRG2*/Col-0 plants, in which MRG2 protein was overexpressed in the WT plants, in response to warm temperatures. As shown in Figures 7F and 7G, the PIF4 protein abundance in the *35S::Flag-MRG2*/Col-0 plants was obviously higher than in WT control, regardless of whether MG132 was applied. Consistently, the *35S::Flag-MRG2*/Col-0 plant displayed a significant increase in the hypocotyl length under warm temperatures compared to WT (Figure 7H). Notably, there is a significant decrease in PIF4 ubiquitination in the *35S::Flag-MRG2*/Col-0 plants, suggesting that the overexpression of MRG2 inhibits the ubiquitination and proteasomal degradation of PIF4 (Figure S9C). The transcripts of *phyB* and phyB proteins were almost unchanged in the *mrg1 mrg2* mutant and *35S::Flag-MRG2*/Col-0 plants compared to WT (Figures 7D–7G, S9D, and S9E), indicating that the altered PIF4 protein in *mrg1 mrg2* and *35S::Flag-MRG2*/Col-0 plants were not due to the different abundance of phyB. In addition, the transcripts of *PIF4* were similar in the WT, *mrg1 mrg2*, and *35S::Flag-MRG2*/Col-0 plants at the same time point under warm conditions (Figure S9E), supporting the notion that the altered protein levels of

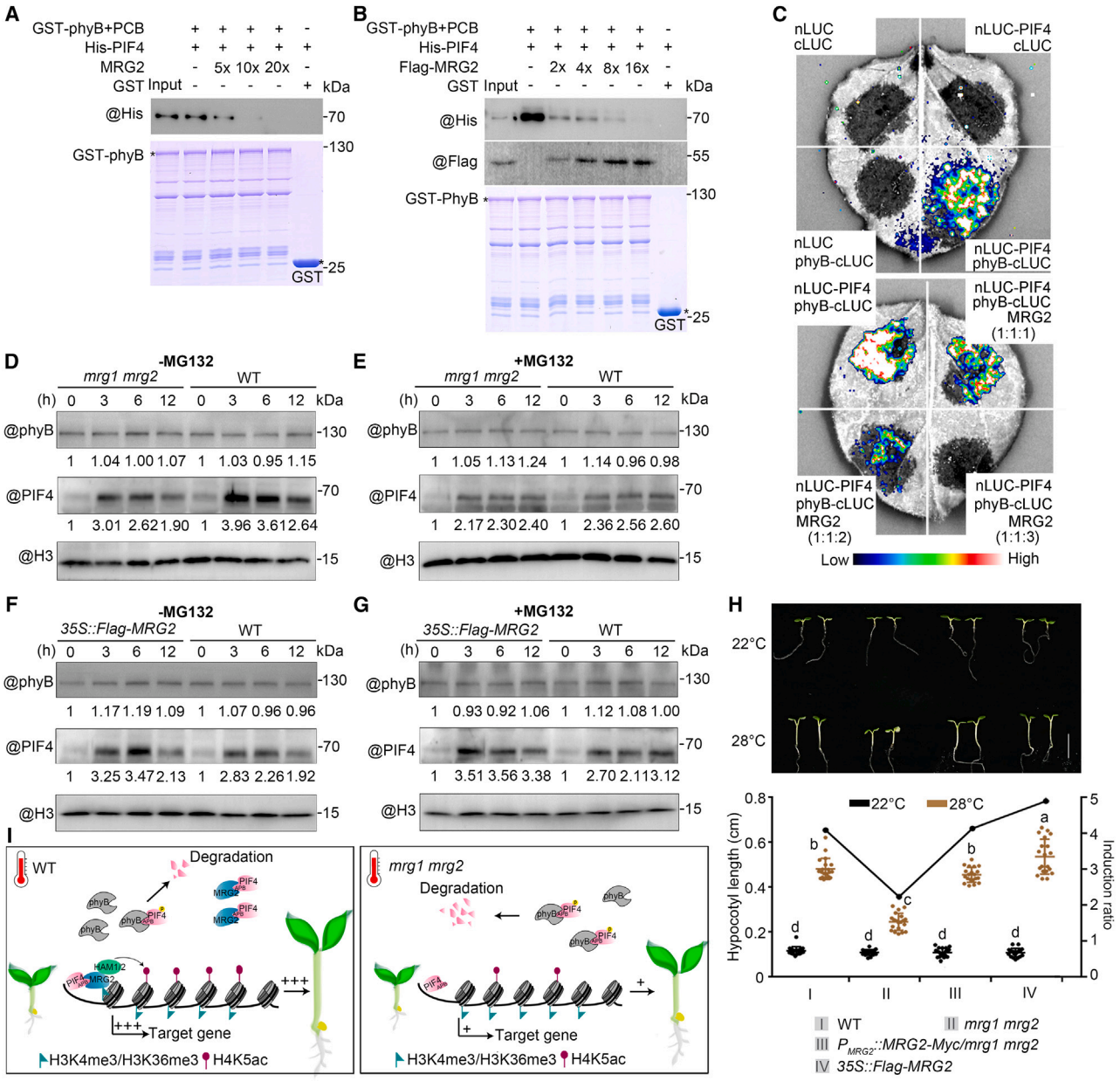

Figure 7. MRG2 competes with phyB to interact with PIF4 and stabilizes the PIF4 protein

(A) Competitive pulldown assay showing that increases in the abundance of purified recombinant MRG2 from *Escherichia coli* gradually inhibited the phyB–PIF4 interaction. His-PIF4 was pulled down and detected in a western blot by using an anti-His antibody. GST-phyB and GST proteins are marked by asterisks in the gel stained with Coomassie brilliant blue. PCB, phycocyanobilin.

(B) Competitive assay using the Flag-MRG2 protein extracted from *35S::Flag-MRG2*/Col-0 plants. His-PIF4 and Flag-MRG2 were detected in a western blot by using anti-His and anti-Flag antibodies, respectively. GST-phyB and GST proteins are marked by asterisks in the gel stained with Coomassie brilliant blue.

(C) Split luciferase assay showing the competition between MRG2 and phyB to interact with PIF4. Tobacco leaves were co-infiltrated with *Agrobacterium* containing nLUC-PIF4 and phyB-cLUC with or without Flag-MRG2. Subsequent luminescence imaging was performed by using a charge-coupled device imaging system.

(D and E) Western blot showing the protein levels of PIF4 and phyB in the *mrg1 mrg2* and WT plants under warm conditions without (D) or with (E) MG132.

(F and G) Western blot showing the protein levels of PIF4 and phyB in the *35S::Flag-MRG2*/Col-0 and WT plants under warm conditions without (F) or with (G) MG132.

(D–G) Plants are grown at 22°C for 6 days and then incubated at 28°C for 0, 3, 6, and 12 h.

(E and G) Plants are treated with 42 μM MG132 for 4 hours before shifting to warm conditions. PIF4 and phyB are analyzed in a western blot by using the anti-PIF4 and anti-phyB antibodies, respectively, with H3 serving as a control for nuclear proteins. Band intensities are determined by using ImageJ and normalized against the H3 band intensity to determine the fold change in protein abundance. For different samples, band intensities are calculated relative to the band at the 0-h time point.

(legend continued on next page)

PIF4 in *mrg1 mrg2* and *35S::Flag-MRG2*/Col-0 were not due to the different levels of *PIF4* mRNA. Taken together, MRG1/2 appeared to stabilize PIF4 by competing with phyB, which positively regulated thermomorphogenesis (Figure 7I).

DISCUSSION

Chromatin regulatory mechanisms modulate multiple biological processes, including responses to environmental changes. As important histone methylation reader proteins, Arabidopsis MRG1/2 regulate various biological processes by interacting with diverse partners. In the present study, we determined that MRG1/2 influence thermomorphogenesis by physically interacting with the central thermoregulator PIF4.

We have previously reported that MRGs interact with PIF7 to promote hypocotyl elongation upon shade avoidance syndrome (SAS) in Arabidopsis.[50] In shade conditions, MRG2 physically interacts with PIF7 and promotes the transcription of multiple downstream PIF7-target genes by increasing H4K5ac.[50] Similarly, MRG2 and PIF4 also bind to the PIF4 target genes to enhance H4K5ac, thereby promoting their transcription under warm conditions, suggesting a conserved regulatory mechanism to promote hypocotyl elongation for both MRG2-PIF4 and MRG2-PIF7. To be noted that the regions of PIF4 and PIF7 responsible for interacting with MRG2 are different (Figure 4).[50] PIF4 interacts with MRG2 through the APB domain (Figures 4E–4G), the same domain responsible for binding to phyB, whereas PIF7 interacts with MRG2 via the region located between the APB and the bHLH domains.[50] The distinct regions within PIF7 responsible for interaction with phyB and MRG2 imply that there may be different mechanisms for MRG2 involved in the regulation of PIF4 and PIF7 at the protein level. Consistently, MRG2 is not able to compete with phyB to bind PIF7 (Figure S9F). PIF7, a major transcription factor involved in SAS,[56,57] has been found to be involved in the thermomorphogenic response.[58,59] Notably, the *pif4* mutant exhibits a more severe warm induced-defective phenotype than that of *pif7*,[60] indicating that PIF4 plays a dominant role in response to warm temperatures, whereas PIF7 functions in thermomorphogenesis particularly in shade conditions, showing a synergistic growth response to both shade and warm temperatures,[60] which is consistent with our observations (Figure S9G). Although both PIF4 and PIF7 proteins accumulate rapidly in response to warm temperatures, they are regulated by different mechanisms. The active Pfr phyB induces the phosphorylation of PIF1/3/4/5, but not PIF7.[37,61–63] Under warm conditions, the reduction in the active Pfr phyB prevents the phosphorylation and subsequent degradation of PIF4, and then more PIF4 protein is released.[33–37] However, PIF7 protein quickly increases due to the enhanced translation of *PIF7* mRNA mediated by the formation of an RNA hairpin within its 5′ UTR in response to warmth.[58] Thus, the warmth-induced accumulations of PIF4 and PIF7 are differently regulated, suggesting that there could be more different regulatory mechanisms for PIF4 and PIF7 in temperature response to be discovered.

In Arabidopsis, the histone deacetylases HDA9, HDA15, and HDA19 are essential for responses to warm ambient conditions because they regulate histone acetylation,[40–42] reflecting the importance of histone acetylation for thermomorphogenesis. A previous study confirmed that MRG1/2 interact with HAM1/2, which are histone H4 acetyltransferases.[48] Consistent with this earlier finding, we observed that the H3K9ac and H4K5ac levels at key thermoresponsive genes increased significantly under warm conditions (Figures 6 and S6E–S6G). Moreover, the increase in the H4K5ac level at 28°C was inhibited in the *mrg1 mrg2* and *pif4* mutants, indicating that the MRG1/2-PIF4 module is necessary for the H4K5ac modification at their target genes. MRG1/2 function as the specific readers for H3K4me3/H3K36me3. In our ChIP-qPCR assay, the lack of MRG1/2 did not alter the H3K4me3 and H3K36me3 levels at the *YUC8* locus (Figures S6B–S6D), suggesting that a short-term exposure to warm conditions (6 h) is insufficient for inducing obvious changes to histone methylations. Compared with histone acetylations, histone methylations are more stable and have a longer turnover time. More specifically, the half-lives of H3K4me3 and H3K36me3 are respectively 6.8 and 57 h in mammalian cells,[64] which are longer than the half-lives of histone acetylations (0.8–2.3 h).[65] Histone acetylations are highly dynamic and may quickly respond to environmental changes, which is in accordance with our results indicating that MRG1/2 along with PIF4 directly target and activate essential thermoresponsive genes by promoting histone acetylations.

In addition to transcriptional regulation, *PIF4* expression is regulated at the posttranslational level (e.g., regulation of PIF4 stability), which is important for thermomorphogenesis. The brassinosteroid signaling-related kinase BIN2 binds to and phosphorylates PIF4 and destabilizes PIF4 at dawn.[26] DET1 reportedly increases the stability of PIFs, including PIF4 in darkness.[27] HMR, which is required for the phyB-mediated sensing of elevated temperatures, promotes the accumulation of PIF4 under warm conditions.[29] Another study demonstrated that SPA regulates thermomorphogenesis by stabilizing PIF4 under warm ambient conditions.[28] More recently, RCB was reported to interact with HMR to stabilize PIF4 during the daytime and initiate thermomorphogenesis.[30] A recently published work shows that heat shock transcription factor 1d stabilizes PIF4 by competing with phyB.[66] However, the molecular mechanisms underlying the stabilizing effects of the above-mentioned regulators on PIF4 remain largely unclear.

In the present study, we examined how MRG proteins stabilize PIF4 (Figure 7I). In WT Arabidopsis, MRG proteins compete with phyB for the binding to PIF4, thereby limiting PIF4 degradation.

(H) Phenotypes of the WT, *mrg1 mrg2*, P_{MRG2}*::MRG2-Myc/mrg1 mrg2*, and *35S::Flag-MRG2* plants treated at 22°C (normal conditions) or 28°C (warm conditions). Scale bar, 0.5 cm. The left y axis presents the hypocotyl length, and the right y axis presents the ratio of the hypocotyl length at 28°C to that at 22°C. The hypocotyl lengths for the indicated genotypes were calculated by using at least 20 plants (one-way ANOVA, followed by Fisher's LSD test; $p < 0.05$).

(I) Working model showing the involvement of MRG1/2-PIF4 in thermomorphogenesis. In WT, MRG2 competes with phyB to interact with PIF4, thereby contributing to the stabilization of PIF4. MRG2-PIF4 directly targets and maintains the hyperacetylation state at the chromatin regions of thermoresponsive genes, such as *YUC8* and *SAUR19*, to activate their transcription to promote the elongation of the hypocotyl upon warm conditions. In *mrg1 mrg2* mutants, the absence of MRG1/2 leads to the instability of the PIF4 protein and inhibits thermomorphogenesis in Arabidopsis.

The MRG-PIF4 complex targets thermoresponsive genes and promotes histone acetylations to activate gene transcription, ultimately leading to hypocotyl elongation in response to warm ambient conditions. In the *mrg1 mrg2* mutant, the lack of MRG1/2 results in the increased binding between phyB and PIF4, the latter of which is subsequently phosphorylated and ultimately degraded via ubiquitin-proteasome-dependent proteolysis. This leads to defective hypocotyl elongation under warm conditions. MRG2 promotes thermomorphogenesis in both transcriptional regulation and posttranscriptional regulation. First, MRG2-PIF4 target to the thermoresponsive genes and promote their transcription by enhancing H4K5ac in a temperature-dependent manner. Second, MRG2 stabilizes PIF4 by competing with phyB, presenting a posttranslational regulation of PIF4 at the protein level. Although the active Pfr phyB is diminished upon warm temperatures,[34] the remaining Pfr phyB can still interact with PIF4 and trigger PIF4 phosphorylation, resulting in the irreversible degradation of PIF4,[33,35,36] whereas the reversible interaction between MRG2 and PIF4 (Figures 7C and S8C) possibly offers a flexible mechanism to regulate PIF4 at the protein level and facilitates appropriate plant responses to the elevated temperatures.

Limitations of the study

Although our work reveals that MRG proteins activate the thermoresponsive genes by inducing histone acetylations and stabilizing PIF4 protein upon warm treatment in Arabidopsis, this study still has limitations. The distribution of MRG2 along the genome in response to warm temperatures is not determined because we could not find a suitable technique to obtain the reliable ChIP-seq data of MRG2. For the ChIP-seq data of H3K9ac and H4K5ac, all of the DNA fragments precipitated by the anti-H3K9ac and anti-H4K5ac antibodies are amplified to construct the libraries for sequencing, so the genes enriched of H3K9ac/H4K5ac modifications will be well amplified, whereas those lowly marked by H3K9ac/H4K5ac are not easily amplified—even easily lost. Compared to those highly expressed genes enriched of acetylation, the levels of H4K5ac at *YUC8*, *SAUR19*, and *PAR1* were much lower (Figure S7), which is why we think that decreased H4K5ac at these genes were not detected at 28°C in the *pif4* mutant compared to WT in our ChIP-seq data.

STAR★METHODS

Detailed methods are provided in the online version of this paper and include the following:

- KEY RESOURCES TABLE
- RESOURCE AVAILABILITY
  - Lead contact
  - Materials availability
  - Data and code availability
- EXPERIMENTAL MODEL AND STUDY PARTICIPANT DETAILS
- METHOD DETAILS
  - Plant growth conditions
  - RNA-seq analysis
  - ChIP-seq analysis
  - qRT-PCR analysis
  - Yeast two-hybrid assay
  - GST pulldown assay
  - Co-IP assay
  - BiFC assay
  - ChIP-qPCR assay
  - Competitive protein binding assay
  - Spilt luciferase assay
  - Protein extraction and western blot assays
- QUANTIFICATION AND STATISTICAL ANALYSIS

SUPPLEMENTAL INFORMATION

Supplemental information can be found online at https://doi.org/10.1016/j.celrep.2024.113726.

ACKNOWLEDGMENTS

We thank Dr. Hongquan Yang for providing the pGEX-4T-1-phyB recombinant plasmid and the *phyB-9* mutant. This work was supported by grants from the National Natural Science Foundation of China (NSFC31930017 and 31800207). We thank Liwen Bianji (Edanz) (www.liwenbianji.cn) for editing the English text of a draft of this manuscript.

AUTHOR CONTRIBUTIONS

A.D. and B.L. conceived and designed the research. N.Z., C.L., N.L., B.W., and J. Wu performed the experiments. W.X. and J. Wang analyzed the RNA-seq and ChIP-seq data. N.Z., B.L., W.S., and A.D. wrote the manuscript. All of the authors read, revised, and approved the manuscript.

DECLARATION OF INTERESTS

The authors declare no competing interests.

Received: September 26, 2022
Revised: October 14, 2023
Accepted: January 15, 2024

REFERENCES

1. Battisti, D.S., and Naylor, R.L. (2009). Historical warnings of future food insecurity with unprecedented seasonal heat. Science *323*, 240–244. https://doi.org/10.1126/science.1164363.
2. Nicotra, A.B., Atkin, O.K., Bonser, S.P., Davidson, A.M., Finnegan, E.J., Mathesius, U., Poot, P., Purugganan, M.D., Richards, C.L., Valladares, F., and van Kleunen, M. (2010). Plant phenotypic plasticity in a changing climate. Trends Plant Sci. *15*, 684–692. https://doi.org/10.1016/j.tplants.2010.09.008.
3. Bellard, C., Bertelsmeier, C., Leadley, P., Thuiller, W., and Courchamp, F. (2012). Impacts of climate change on the future of biodiversity. Ecol. Lett. *15*, 365–377. https://doi.org/10.1111/j.1461-0248.2011.01736.x.
4. Balasubramanian, S., Sureshkumar, S., Lempe, J., and Weigel, D. (2006). Potent induction of Arabidopsis thaliana flowering by elevated growth temperature. PLoS Genet. *2*, e106. https://doi.org/10.1371/journal.pgen.0020106.
5. Quint, M., Delker, C., Franklin, K.A., Wigge, P.A., Halliday, K.J., and van Zanten, M. (2016). Molecular and genetic control of plant thermomorphogenesis. Nat. Plants *2*, 15190. https://doi.org/10.1038/nplants.2015.190.
6. Crawford, A.J., McLachlan, D.H., Hetherington, A.M., and Franklin, K.A. (2012). High temperature exposure increases plant cooling capacity. Curr. Biol. *22*, R396–R397. https://doi.org/10.1016/j.cub.2012.03.044.

7. Casal, J.J., and Balasubramanian, S. (2019). Thermomorphogenesis. Annu. Rev. Plant Biol. *70*, 321–346. https://doi.org/10.1146/annurev-arplant-050718-095919.

8. Huq, E., and Quail, P.H. (2002). PIF4, a phytochrome-interacting bHLH factor, functions as a negative regulator of phytochrome B signaling in Arabidopsis. EMBO J. *21*, 2441–2450. https://doi.org/10.1093/emboj/21.10.2441.

9. Leivar, P., and Quail, P.H. (2011). PIFs: pivotal components in a cellular signaling hub. Trends Plant Sci. *16*, 19–28. https://doi.org/10.1016/j.tplants.2010.08.003.

10. Franklin, K.A., Lee, S.H., Patel, D., Kumar, S.V., Spartz, A.K., Gu, C., Ye, S., Yu, P., Breen, G., Cohen, J.D., et al. (2011). Phytochrome-interacting factor 4 (PIF4) regulates auxin biosynthesis at high temperature. Proc. Natl. Acad. Sci. USA *108*, 20231–20235. https://doi.org/10.1073/pnas.1110682108.

11. Koini, M.A., Alvey, L., Allen, T., Tilley, C.A., Harberd, N.P., Whitelam, G.C., and Franklin, K.A. (2009). High temperature-mediated adaptations in plant architecture require the bHLH transcription factor PIF4. Curr. Biol. *19*, 408–413. https://doi.org/10.1016/j.cub.2009.01.046.

12. Bou-Torrent, J., Roig-Villanova, I., Galstyan, A., and Martínez-García, J.F. (2008). PAR1 and PAR2 integrate shade and hormone transcriptional networks. Plant Signal. Behav. *3*, 453–454. https://doi.org/10.4161/psb.3.7.5599.

13. Gray, W.M., Ostin, A., Sandberg, G., Romano, C.P., and Estelle, M. (1998). High temperature promotes auxin-mediated hypocotyl elongation in Arabidopsis. Proc. Natl. Acad. Sci. USA *95*, 7197–7202. https://doi.org/10.1073/pnas.95.12.7197.

14. Leivar, P., Tepperman, J.M., Cohn, M.M., Monte, E., Al-Sady, B., Erickson, E., and Quail, P.H. (2012). Dynamic antagonism between phytochromes and PIF family basic helix-loop-helix factors induces selective reciprocal responses to light and shade in a rapidly responsive transcriptional network in Arabidopsis. Plant Cell *24*, 1398–1419. https://doi.org/10.1105/tpc.112.095711.

15. Stavang, J.A., Gallego-Bartolomé, J., Gómez, M.D., Yoshida, S., Asami, T., Olsen, J.E., García-Martínez, J.L., Alabadí, D., and Blázquez, M.A. (2009). Hormonal regulation of temperature-induced growth in Arabidopsis. Plant J. *60*, 589–601. https://doi.org/10.1111/j.1365-313X.2009.03983.x.

16. Sun, J., Qi, L., Li, Y., Chu, J., and Li, C. (2012). PIF4-mediated activation of YUCCA8 expression integrates temperature into the auxin pathway in regulating arabidopsis hypocotyl growth. PLoS Genet. *8*, e1002594. https://doi.org/10.1371/journal.pgen.1002594.

17. Nozue, K., Covington, M.F., Duek, P.D., Lorrain, S., Fankhauser, C., Harmer, S.L., and Maloof, J.N. (2007). Rhythmic growth explained by coincidence between internal and external cues. Nature *448*, 358–361. https://doi.org/10.1038/nature05946.

18. Nusinow, D.A., Helfer, A., Hamilton, E.E., King, J.J., Imaizumi, T., Schultz, T.F., Farré, E.M., and Kay, S.A. (2011). The ELF4-ELF3-LUX complex links the circadian clock to diurnal control of hypocotyl growth. Nature *475*, 398–402. https://doi.org/10.1038/nature10182.

19. Delker, C., Sonntag, L., James, G.V., Janitza, P., Ibañez, C., Ziermann, H., Peterson, T., Denk, K., Mull, S., Ziegler, J., et al. (2014). The DET1-COP1-HY5 pathway constitutes a multipurpose signaling module regulating plant photomorphogenesis and thermomorphogenesis. Cell Rep. *9*, 1983–1989. https://doi.org/10.1016/j.celrep.2014.11.043.

20. Lee, J., He, K., Stolc, V., Lee, H., Figueroa, P., Gao, Y., Tongprasit, W., Zhao, H., Lee, I., and Deng, X.W. (2007). Analysis of transcription factor HY5 genomic binding sites revealed its hierarchical role in light regulation of development. Plant Cell *19*, 731–749. https://doi.org/10.1105/tpc.106.047688.

21. Nieto, C., López-Salmerón, V., Davière, J.M., and Prat, S. (2015). ELF3-PIF4 interaction regulates plant growth independently of the Evening Complex. Curr. Biol. *25*, 187–193. https://doi.org/10.1016/j.cub.2014.10.070.

22. Zhu, J.Y., Oh, E., Wang, T., and Wang, Z.Y. (2016). TOC1-PIF4 interaction mediates the circadian gating of thermoresponsive growth in Arabidopsis. Nat. Commun. *7*, 13692. https://doi.org/10.1038/ncomms13692.

23. Song, Z., Heng, Y., Bian, Y., Xiao, Y., Liu, J., Zhao, X., Jiang, Y., Deng, X.W., and Xu, D. (2021). BBX11 promotes red light-mediated photomorphogenic development by modulating phyB-PIF4 signaling. aBIOTECH *2*, 117–130. https://doi.org/10.1007/s42994-021-00037-2.

24. Zhang, B., Holmlund, M., Lorrain, S., Norberg, M., Bakó, L., Fankhauser, C., and Nilsson, O. (2017). BLADE-ON-PETIOLE proteins act in an E3 ubiquitin ligase complex to regulate PHYTOCHROME INTERACTING FACTOR 4 abundance. Elife *6*, e26759. https://doi.org/10.7554/eLife.26759.

25. de Lucas, M., Davière, J.M., Rodríguez-Falcón, M., Pontin, M., Iglesias-Pedraz, J.M., Lorrain, S., Fankhauser, C., Blázquez, M.A., Titarenko, E., and Prat, S. (2008). A molecular framework for light and gibberellin control of cell elongation. Nature *451*, 480–484. https://doi.org/10.1038/nature06520.

26. Bernardo-García, S., de Lucas, M., Martínez, C., Espinosa-Ruiz, A., Davière, J.M., and Prat, S. (2014). BR-dependent phosphorylation modulates PIF4 transcriptional activity and shapes diurnal hypocotyl growth. Genes Dev. *28*, 1681–1694. https://doi.org/10.1101/gad.243675.114.

27. Dong, J., Tang, D., Gao, Z., Yu, R., Li, K., He, H., Terzaghi, W., Deng, X.W., and Chen, H. (2014). Arabidopsis DE-ETIOLATED1 represses photomorphogenesis by positively regulating phytochrome-interacting factors in the dark. Plant Cell *26*, 3630–3645. https://doi.org/10.1105/tpc.114.130666.

28. Lee, S., Paik, I., and Huq, E. (2020). SPAs promote thermomorphogenesis by regulating the phyB-PIF4 module in Arabidopsis. Development *147*. https://doi.org/10.1242/dev.189233.

29. Qiu, Y., Li, M., Kim, R.J.A., Moore, C.M., and Chen, M. (2019). Daytime temperature is sensed by phytochrome B in Arabidopsis through a transcriptional activator HEMERA. Nat. Commun. *10*, 140. https://doi.org/10.1038/s41467-018-08059-z.

30. Qiu, Y., Pasoreck, E.K., Yoo, C.Y., He, J., Wang, H., Bajracharya, A., Li, M., Larsen, H.D., Cheung, S., and Chen, M. (2021). RCB initiates Arabidopsis thermomorphogenesis by stabilizing the thermoregulator PIF4 in the daytime. Nat. Commun. *12*, 2042. https://doi.org/10.1038/s41467-021-22313-x.

31. Han, X., Yu, H., Yuan, R., Yang, Y., An, F., and Qin, G. (2019). Arabidopsis Transcription Factor TCP5 Controls Plant Thermomorphogenesis by Positively Regulating PIF4 Activity. iScience *15*, 611–622. https://doi.org/10.1016/j.isci.2019.04.005.

32. Yan, Y., Li, C., Dong, X., Li, H., Zhang, D., Zhou, Y., Jiang, B., Peng, J., Qin, X., Cheng, J., et al. (2020). MYB30 Is a Key Negative Regulator of Arabidopsis Photomorphogenic Development That Promotes PIF4 and PIF5 Protein Accumulation in the Light. Plant Cell *32*, 2196–2215. https://doi.org/10.1105/tpc.19.00645.

33. Jung, J.H., Domijan, M., Klose, C., Biswas, S., Ezer, D., Gao, M., Khattak, A.K., Box, M.S., Charoensawan, V., Cortijo, S., et al. (2016). Phytochromes function as thermosensors in Arabidopsis. Science *354*, 886–889. https://doi.org/10.1126/science.aaf6005.

34. Legris, M., Klose, C., Burgie, E.S., Rojas, C.C.R., Neme, M., Hiltbrunner, A., Wigge, P.A., Schäfer, E., Vierstra, R.D., and Casal, J.J. (2016). Phytochrome B integrates light and temperature signals in Arabidopsis. Science *354*, 897–900. https://doi.org/10.1126/science.aaf5656.

35. Li, H., Burgie, E.S., Gannam, Z.T.K., Li, H., and Vierstra, R.D. (2022). Plant phytochrome B is an asymmetric dimer with unique signalling potential. Nature *604*, 127–133. https://doi.org/10.1038/s41586-022-04529-z.

36. Quail, P.H. (2002). Phytochrome photosensory signalling networks. Nat. Rev. Mol. Cell Biol. *3*, 85–93. https://doi.org/10.1038/nrm728.

37. Lorrain, S., Allen, T., Duek, P.D., Whitelam, G.C., and Fankhauser, C. (2008). Phytochrome-mediated inhibition of shade avoidance involves

degradation of growth-promoting bHLH transcription factors. Plant J. *53*, 312–323. https://doi.org/10.1111/j.1365-313X.2007.03341.x.

38. Kumar, S.V., and Wigge, P.A. (2010). H2A.Z-containing nucleosomes mediate the thermosensory response in Arabidopsis. Cell *140*, 136–147. https://doi.org/10.1016/j.cell.2009.11.006.

39. Xue, M., Zhang, H., Zhao, F., Zhao, T., Li, H., and Jiang, D. (2021). The INO80 chromatin remodeling complex promotes thermomorphogenesis by connecting H2A.Z eviction and active transcription in Arabidopsis. Mol. Plant *14*, 1799–1813. https://doi.org/10.1016/j.molp.2021.07.001.

40. Shen, Y., Lei, T., Cui, X., Liu, X., Zhou, S., Zheng, Y., Guérard, F., Issakidis-Bourguet, E., and Zhou, D.X. (2019). Arabidopsis histone deacetylase HDA15 directly represses plant response to elevated ambient temperature. Plant J. *100*, 991–1006. https://doi.org/10.1111/tpj.14492.

41. Tasset, C., Singh Yadav, A., Sureshkumar, S., Singh, R., van der Woude, L., Nekrasov, M., Tremethick, D., van Zanten, M., and Balasubramanian, S. (2018). POWERDRESS-mediated histone deacetylation is essential for thermomorphogenesis in Arabidopsis thaliana. PLoS Genet. *14*, e1007280. https://doi.org/10.1371/journal.pgen.1007280.

42. van der Woude, L.C., Perrella, G., Snoek, B.L., van Hoogdalem, M., Novák, O., van Verk, M.C., van Kooten, H.N., Zorn, L.E., Tonckens, R., Dongus, J.A., et al. (2019). HISTONE DEACETYLASE 9 stimulates auxin-dependent thermomorphogenesis in Arabidopsis thaliana by mediating H2A.Z depletion. Proc. Natl. Acad. Sci. USA *116*, 25343–25354. https://doi.org/10.1073/pnas.1911694116.

43. He, K., Mei, H., Zhu, J., Qiu, Q., Cao, X., and Deng, X. (2022). The histone H3K27 demethylase REF6/JMJ12 promotes thermomorphogenesis in Arabidopsis. Natl. Sci. Rev. *9*, nwab213. https://doi.org/10.1093/nsr/nwab213.

44. Zha, P., Jing, Y., Xu, G., and Lin, R. (2017). PICKLE chromatin-remodeling factor controls thermosensory hypocotyl growth of Arabidopsis. Plant Cell Environ. *40*, 2426–2436. https://doi.org/10.1111/pce.13049.

45. Cui, X., Zheng, Y., Lu, Y., Issakidis-Bourguet, E., and Zhou, D.X. (2021). Metabolic control of histone demethylase activity involved in plant response to high temperature. Plant Physiol. *185*, 1813–1828. https://doi.org/10.1093/plphys/kiab020.

46. Bu, Z., Yu, Y., Li, Z., Liu, Y., Jiang, W., Huang, Y., and Dong, A.W. (2014). Regulation of arabidopsis flowering by the histone mark readers MRG1/2 via interaction with CONSTANS to modulate FT expression. PLoS Genet. *10*, e1004617. https://doi.org/10.1371/journal.pgen.1004617.

47. An, Z., Yin, L., Liu, Y., Peng, M., Shen, W.H., and Dong, A. (2020). The histone methylation readers MRG1/MRG2 and the histone chaperones NRP1/NRP2 associate in fine-tuning Arabidopsis flowering time. Plant J. *103*, 1010–1024. https://doi.org/10.1111/tpj.14780.

48. Xu, Y., Gan, E.S., Zhou, J., Wee, W.Y., Zhang, X., and Ito, T. (2014). Arabidopsis MRG domain proteins bridge two histone modifications to elevate expression of flowering genes. Nucleic Acids Res. *42*, 10960–10974. https://doi.org/10.1093/nar/gku781.

49. Guo, Z., Li, Z., Liu, Y., An, Z., Peng, M., Shen, W.H., Dong, A., and Yu, Y. (2020). MRG1/2 histone methylation readers and HD2C histone deacetylase associate in repression of the florigen gene FT to set a proper flowering time in response to day-length changes. New Phytol. *227*, 1453–1466. https://doi.org/10.1111/nph.16616.

50. Peng, M., Li, Z., Zhou, N., Ma, M., Jiang, Y., Dong, A., Shen, W.H., and Li, L. (2018). Linking PHYTOCHROME-INTERACTING FACTOR to Histone Modification in Plant Shade Avoidance. Plant Physiol. *176*, 1341–1351. https://doi.org/10.1104/pp.17.01189.

51. Lu, H.P., Wang, J.J., Wang, M.J., and Liu, J.X. (2021). Roles of plant hormones in thermomorphogenesis. Stress Biol. *1*, 20. https://doi.org/10.1007/s44154-021-00022-1.

52. Xu, Y., and Zhu, Z. (2021). PIF4 and PIF4-Interacting Proteins: At the Nexus of Plant Light, Temperature and Hormone Signal Integrations. Int. J. Mol. Sci. *22*, 10304. https://doi.org/10.3390/ijms221910304.

53. Khanna, R., Huq, E., Kikis, E.A., Al-Sady, B., Lanzatella, C., and Quail, P.H. (2004). A novel molecular recognition motif necessary for targeting photoactivated phytochrome signaling to specific basic helix-loop-helix transcription factors. Plant Cell *16*, 3033–3044. https://doi.org/10.1105/tpc.104.025643.

54. Sun, J., Qi, L., Li, Y., Zhai, Q., and Li, C. (2013). PIF4 and PIF5 transcription factors link blue light and auxin to regulate the phototropic response in Arabidopsis. Plant Cell *25*, 2102–2114. https://doi.org/10.1105/tpc.113.112417.

55. Kikis, E.A., Oka, Y., Hudson, M.E., Nagatani, A., and Quail, P.H. (2009). Residues clustered in the light-sensing knot of phytochrome B are necessary for conformer-specific binding to signaling partner PIF3. PLoS Genet. *5*, e1000352. https://doi.org/10.1371/journal.pgen.1000352.

56. Galvão, V.C., Fiorucci, A.S., Trevisan, M., Franco-Zorilla, J.M., Goyal, A., Schmid-Siegert, E., Solano, R., and Fankhauser, C. (2019). PIF transcription factors link a neighbor threat cue to accelerated reproduction in Arabidopsis. Nat. Commun. *10*, 4005. https://doi.org/10.1038/s41467-019-11882-7.

57. Li, L., Ljung, K., Breton, G., Schmitz, R.J., Pruneda-Paz, J., Cowing-Zitron, C., Cole, B.J., Ivans, L.J., Pedmale, U.V., Jung, H.S., et al. (2012). Linking photoreceptor excitation to changes in plant architecture. Genes Dev. *26*, 785–790. https://doi.org/10.1101/gad.187849.112.

58. Chung, B.Y.W., Balcerowicz, M., Di Antonio, M., Jaeger, K.E., Geng, F., Franaszek, K., Marriott, P., Brierley, I., Firth, A.E., and Wigge, P.A. (2020). An RNA thermoswitch regulates daytime growth in Arabidopsis. Nat. Plants *6*, 522–532. https://doi.org/10.1038/s41477-020-0633-3.

59. Fiorucci, A.S., Galvão, V.C., Ince, Y.Ç., Boccaccini, A., Goyal, A., Allenbach Petrolati, L., Trevisan, M., and Fankhauser, C. (2020). PHYTOCHROME INTERACTING FACTOR 7 is important for early responses to elevated temperature in Arabidopsis seedlings. New Phytol. *226*, 50–58. https://doi.org/10.1111/nph.16316.

60. Burko, Y., Willige, B.C., Seluzicki, A., Novák, O., Ljung, K., and Chory, J. (2022). PIF7 is a master regulator of thermomorphogenesis in shade. Nat. Commun. *13*, 4942. https://doi.org/10.1038/s41467-022-32585-6.

61. Al-Sady, B., Ni, W., Kircher, S., Schäfer, E., and Quail, P.H. (2006). Photoactivated phytochrome induces rapid PIF3 phosphorylation prior to proteasome-mediated degradation. Mol. Cell *23*, 439–446. https://doi.org/10.1016/j.molcel.2006.06.011.

62. Shen, H., Moon, J., and Huq, E. (2005). PIF1 is regulated by light-mediated degradation through the ubiquitin-26S proteasome pathway to optimize photomorphogenesis of seedlings in Arabidopsis. Plant J. *44*, 1023–1035. https://doi.org/10.1111/j.1365-313X.2005.02606.x.

63. Shen, Y., Khanna, R., Carle, C.M., and Quail, P.H. (2007). Phytochrome induces rapid PIF5 phosphorylation and degradation in response to red-light activation. Plant Physiol. *145*, 1043–1051. https://doi.org/10.1104/pp.107.105601.

64. Zheng, Y., Tipton, J.D., Thomas, P.M., Kelleher, N.L., and Sweet, S.M.M. (2014). Site-specific human histone H3 methylation stability: fast K4me3 turnover. Proteomics *14*, 2190–2199. https://doi.org/10.1002/pmic.201400060.

65. Zheng, Y., Thomas, P.M., and Kelleher, N.L. (2013). Measurement of acetylation turnover at distinct lysines in human histones identifies long-lived acetylation sites. Nat. Commun. *4*, 2203. https://doi.org/10.1038/ncomms3203.

66. Tan, W., Chen, J., Yue, X., Chai, S., Liu, W., Li, C., Yang, F., Gao, Y., Gutiérrez Rodríguez, L., Resco de Dios, V., et al. (2023). The heat response regulators HSFA1s promote Arabidopsis thermomorphogenesis via stabilizing PIF4 during the day. Sci. Adv. *9*, eadh1738. https://doi.org/10.1126/sciadv.adh1738.

67. Xu, F., He, S., Zhang, J., Mao, Z., Wang, W., Li, T., Hua, J., Du, S., Xu, P., Li, L., et al. (2018). Photoactivated CRY1 and phyB Interact Directly with AUX/IAA Proteins to Inhibit Auxin Signaling in Arabidopsis. Mol. Plant *11*, 523–541. https://doi.org/10.1016/j.molp.2017.12.003.

68. Martin, M. (2011). Cutadapt removes adapter sequences from high-throughput sequencing reads. EMBnet. j. *17*, 10–12. https://doi.org/10.14806/EJ.17.1.200.

69. Kim, D., Langmead, B., and Salzberg, S.L. (2015). HISAT: a fast spliced aligner with low memory requirements. Nat. Methods *12*, 357–360. https://doi.org/10.1038/nmeth.3317.

70. Li, H., Handsaker, B., Wysoker, A., Fennell, T., Ruan, J., Homer, N., Marth, G., Abecasis, G., and Durbin, R.; 1000 Genome Project Data Processing Subgroup (2009). The Sequence Alignment/Map format and SAMtools. Bioinformatics *25*, 2078–2079. https://doi.org/10.1093/bioinformatics/btp352.

71. Liao, Y., Smyth, G.K., and Shi, W. (2014). featureCounts: an efficient general purpose program for assigning sequence reads to genomic features. Bioinformatics *30*, 923–930. https://doi.org/10.1093/bioinformatics/btt656.

72. Love, M.I., Huber, W., and Anders, S. (2014). Moderated estimation of fold change and dispersion for RNA-seq data with DESeq2. Genome Biol. *15*, 550. https://doi.org/10.1186/s13059-014-0550-8.

73. Ramírez, F., Ryan, D.P., Grüning, B., Bhardwaj, V., Kilpert, F., Richter, A.S., Heyne, S., Dündar, F., and Manke, T. (2016). deepTools2: a next generation web server for deep-sequencing data analysis. Nucleic Acids Res. *44*, W160–W165. https://doi.org/10.1093/nar/gkw257.

74. Thorvaldsdóttir, H., Robinson, J.T., and Mesirov, J.P. (2013). Integrative Genomics Viewer (IGV): high-performance genomics data visualization and exploration. Briefings Bioinf. *14*, 178–192. https://doi.org/10.1093/bib/bbs017.

75. Langmead, B., and Salzberg, S.L. (2012). Fast gapped-read alignment with Bowtie 2. Nat. Methods *9*, 357–359. https://doi.org/10.1038/nmeth.1923.

76. Zhang, Y., Liu, T., Meyer, C.A., Eeckhoute, J., Johnson, D.S., Bernstein, B.E., Nusbaum, C., Myers, R.M., Brown, M., Li, W., and Liu, X.S. (2008). Model-based analysis of ChIP-Seq (MACS). Genome Biol. *9*, R137. https://doi.org/10.1186/gb-2008-9-9-r137.

77. Shao, Z., Zhang, Y., Yuan, G.C., Orkin, S.H., and Waxman, D.J. (2012). MAnorm: a robust model for quantitative comparison of ChIP-Seq data sets. Genome Biol. *13*, R16. https://doi.org/10.1186/gb-2012-13-3-r16.

78. Zhu, L.J., Gazin, C., Lawson, N.D., Pagès, H., Lin, S.M., Lapointe, D.S., and Green, M.R. (2010). ChIPpeakAnno: a Bioconductor package to annotate ChIP-seq and ChIP-chip data. BMC Bioinf. *11*, 237. https://doi.org/10.1186/1471-2105-11-237.

79. Chen, K., Du, K., Shi, Y., Yin, L., Shen, W.H., Yu, Y., Liu, B., and Dong, A. (2021). H3K36 methyltransferase SDG708 enhances drought tolerance by promoting abscisic acid biosynthesis in rice. New Phytol. *230*, 1967–1984. https://doi.org/10.1111/nph.17290.

80. Wang, B., Luo, Q., Li, Y., Du, K., Wu, Z., Li, T., Shen, W.H., Huang, C.H., Gan, J., and Dong, A. (2022). Structural insights into partner selection for MYB and bHLH transcription factor complexes. Nat. Plants *8*, 1108–1117. https://doi.org/10.1038/s41477-022-01223-w.

81. Jang, I.C., Henriques, R., Seo, H.S., Nagatani, A., and Chua, N.H. (2010). Arabidopsis PHYTOCHROME INTERACTING FACTOR proteins promote phytochrome B polyubiquitination by COP1 E3 ligase in the nucleus. Plant Cell *22*, 2370–2383. https://doi.org/10.1105/tpc.109.072520.

STAR★METHODS

KEY RESOURCES TABLE

REAGENT or RESOURCE	SOURCE	IDENTIFIER
Antibodies		
Mouse monoclonal anti-His	GNI	Cat# GNI4110-HS; RRID: AB_3076245
Rabbit polyclonal anti-HA	Abcam	Cat# ab9110; RRID:AB_307019
Mouse monoclonal anti-Flag	Sigma-Aldrich	Cat# F1804; RRID:AB_262044
Rabbit polyclonal anti-H4K5ac	Sigma-Aldrich	Cat# 07-327; RRID:AB_310523
Rabbit polyclonal anti-H3K9ac	Abcam	Cat# ab10812; RRID:AB_297491
Rabbit polyclonal anti-H3K36ac	Active Motif	Cat# 39379; RRID:AB_2614977
Rabbit polyclonal anti-H3K4me3	Abcam	Cat# ab8580; RRID:AB_306649
Rabbit polyclonal anti-H3K36me3	Abcam	Cat# ab9050; RRID:AB_306966
Mouse monoclonal anti-Myc	Abmart	Cat# M20002L: RRID:AB_2861172
Mouse monoclonal anti-phyB	PHYTOAB	Cat# PHY1733; RRID:AB_3076246
Mouse monoclonal anti-HA	Abmart	Cat# M20003M; RRID:AB_2864345
Mouse monoclonal anti-Flag	Abmart	Cat# M20008M; RRID:AB_2713960
Rabbit polyclonal anti-H3	Abcam	Cat# ab1791; RRID:AB_302613
Rabbit Polyclonal anti-PIF4	Abiocode	Cat# R2534-4
Rabbit Monoclonal anti-ubiquitin	Beyotime	Cat# AF1705; RRID:AB_2858211
Bacterial and virus strains		
GV3101 Chemically Competent Cell	WeidiBio	Cat# AC1001
Y2HGold Chemically Competent Cell	WeidiBio	Cat# YC1002
Rosetta(DE3) Chemically Competent Cell	WeidiBio	Cat# EC1010
Chemicals, peptides, and recombinant proteins		
Protein-A Dynabeads	Invitrogen	Cat# 10002D
Proteinase K	Invitrogen	Cat# AM2546
Dr. GenTLE^{TM} Precipitation Carrier	TaKaRa	Cat# 9094
Critical commercial assays		
RNAprep Pure Plant Kit	TIANGEN	Cat# DP432
KAPA Stranded RNA-Seq Kit	Roche	Cat# KK8401
Deposited data		
RNA-seq of WT, *mrg1 mrg2*, *pif4*, and *mrg1 mrg2 pif4* at 22°C and 28°C	This study	GEO：GSE213025
ChIP-seq of P_{PIF4}::*PIF4-HA*/*pif4* at 22°C and 28°C	This study	GEO：GSE242309
ChIP-seq of H3K9ac and H4K5ac in WT and *pif4* at 22°C and 28°C	This study	GEO：GSE252996
Experimental models: Organisms/strains		
Arabidopsis: *Col-0*	Bu et al., 2014[46]	N/A
Arabidopsis: *mrg1*	Bu et al., 2014[46]	N/A
Arabidopsis: *mrg2*	Bu et al., 2014[46]	N/A
Arabidopsis: *mrg1 mrg2*	Bu et al., 2014[46]	N/A
Arabidopsis: *pif4-101*	Lorrain et al., 2008[37]	N/A
Arabidopsis: *phyB-9*	Xu et al., 2018[67]	N/A
Arabidopsis: *mrg1 mrg2 pif4-101*	This study	N/A
Arabidopsis: P_{PIF4}::*PIF4-HA*/*pif4*	This study	N/A
Arabidopsis: P_{MRG2}::*MRG2-Myc*/*mrg1 mrg2*	This study	N/A

(*Continued on next page*)

Continued		
REAGENT or RESOURCE	SOURCE	IDENTIFIER
Arabidopsis: P_{MRG2}::MRG2-Myc/*mrg1 mrg2 pif4-101*	This study	N/A
Arabidopsis: *35S::Flag-MRG2/Col-0*	An et al., 2020[47]	N/A
Arabidopsis: *35S::PIF4-HA/Col-0*	This study	N/A
Oligonucleotides		
Primers are listed in Table S1	This study	N/A
Recombinant DNA		
P_{MRG2}::MRG2-Myc	This study	N/A
P_{PIF4}::PIF4-HA	This study	N/A
AD-PIF4	This study	N/A
BD-MRG2	This study	N/A
GST-PIF4	This study	N/A
GST-PIF4-N1	This study	N/A
GST-PIF4-N2	This study	N/A
GST-PIF4-C1	This study	N/A
GST-PIF4-C2	This study	N/A
His-MRG2	Bu et al., 2014[46]	N/A
GST-MRG1	This study	N/A
GST-MRG2	This study	N/A
His-PIF4	This study	N/A
GST-phyB	This study	N/A
pCold-phyB	This study	N/A
MBP-phyB	This study	N/A
His-PIF7	This study	N/A
MRG2-nYFP	This study	N/A
PIF4-cYFP	This study	N/A
PIF4-N1-cYFP	This study	N/A
PIF4-C2-cYFP	This study	N/A
35S::PIF4-HA	This study	N/A
35S::Flag-MRG2	An et al., 2020[47]	N/A
nLuc-PIF4	This study	N/A
cLuc-phyB	This study	N/A
phyB-Myc	This study	N/A
phyB-G111D	This study	N/A
cLuc-MRG2	This study	N/A
Software and algorithms		
Cutadapt (v.3.5)	Martin, 2011[68]	N/A
HISAT2 (v.2.2.1)	Kim et al., 2015[69]	N/A
SAMtools (v.1.13)	Li et al., 2009[70]	N/A
FeatureCounts (v.2.0.1)	Liao et al., 2014[71]	N/A
DESeq2 (v.1.32.0)	Love et al., 2014[72]	N/A
bamCoverage (v.3.5.1)	Ramirez et al., 2016[73]	N/A
IGV (v.2.11.2)	Thorvaldsdottir et al., 2013[74]	N/A
Bowtie2 (v.2.4.5)	Langmead and Salzberg, 2012[75]	N/A
MACS2 (v.2.2.7.1)	Zhang et al., 2008[76]	N/A
MAnorm (v.1.3.0)	Shao et al., 2012[77]	N/A
ChIPpeakAnno (v.3.28.1)	Zhu et al., 2010[78]	N/A
computeMatrix (v.3.5.1)	Ramirez et al., 2016[73]	N/A
plotHeatmap (v.3.5.1)	Ramirez et al., 2016[73]	N/A

RESOURCE AVAILABILITY

Lead contact

Further information and requests for resources and reagents should be directed to and will be fulfilled by the lead contact, Aiwu Dong (aiwudong@fudan.edu.cn).

Materials availability

Plant materials and plasmids generated in this study will be available upon request. This study did not generate new unique reagents.

Data and code availability

- The RNA-seq data and ChIP-seq data are available online (https://www.ncbi.nlm.nih.gov/geo/; accession number: GSE213025, GSE242309 and GSE252996).
- This paper does not report original code.
- Any additional information required to reanalyze the data reported in this work paper is available from the lead contact upon request.

EXPERIMENTAL MODEL AND STUDY PARTICIPANT DETAILS

All Arabidopsis plants used in this study had the *Columbia-0* genetic background. The *mrg1* (SALK_057762), *mrg2* (SK28487), and *pif4-101* (Garlic_114_G06) mutants were described previously.[37,46] The *35S::Flag-MRG2*/Col-0 transgenic lines were described previously.[47]

To generate P_{PIF4}*::PIF4-HA/pif4*, P_{MRG2}*::MRG2-Myc/mrg1 mrg2*, and P_{MRG2}*::MRG2-Myc/mrg1 mrg2 pif4* plants, the *PIF4* and *MRG2* genomic sequence was amplified by PCR using primers listed in Table S1. The amplified fragment was fused to the sequence encoding HA and Myc, respectively, then inserted into the pCAMBIA1300 vector (Cambia). The *pif4* mutants were transformed with the resulting recombinant plasmid containing the P_{PIF4}*::PIF4-HA* construct. P_{MRG2}*::MRG2-Myc* was used for transforming into the *mrg1 mrg2*. The hypocotyl phenotype of *mrg1 mrg2* was fully rescued by expressing *MRG2* driven by *MRG2* native promoters in five independent lines. P_{MRG2}*::MRG2-Myc/mrg1 mrg2 #5-4* was selected for the following experiments. P_{MRG2}*::MRG2-Myc/mrg1 mrg2 pif4* was generated by crossing the P_{MRG2}*::MRG2-Myc/mrg1 mrg2 #5-4* plant with *mrg1 mrg2 pif4* triple mutant.

To generate the *35S::PIF4-HA*, the full-length *PIF4* cDNA sequence with the *HA* epitope tag was amplified by PCR using specific primers (Table S1) and then cloned into the pCAMBIA1300 vector to generate the *35S::PIF4-HA* construct. The recombinant plasmids were inserted into WT Arabidopsis. The *35S::PIF4-HA/35S::Flag-MRG2* plants were generated via a hybridization.

METHOD DETAILS

Plant growth conditions

Seeds were surface-sterilized by immersing them in 70% ethanol containing 0.02% Tween 20 for 10 min and then in 96% ethanol (three times for 5 min each). All seeds were placed on half-strength Murashige and Skoog (MS) medium (pH 5.7) solidified with 1% agar in plates. After a 2-day stratification at 4°C, the plates were transferred to a growth chamber and maintained under continuous white light (55 $\mu E\ m^{-2}\ s^{-1}$) at 22°C with 60% humidity. To measure the hypocotyl length, petiole length, and leaf hyponasty response, seedlings were grown at 22°C for 4 days and then shifted to 28°C for 3 days (60% humidity, 55 $\mu E\ m^{-2}\ s^{-1}$). Seedlings grown at 22°C for 3 days served as the controls.

RNA-seq analysis

Seedlings were grown on half-strength MS solid medium under continuous white light at 22°C for 6 days. They were then incubated for 3 h at 28°C (warm conditions) or 22°C (normal conditions). Total RNA was extracted from the seedlings using the RNAprep Pure Plant Kit (Tiangen Biotech, Beijing, China). The RNA-seq libraries were constructed according to the instructions of the KAPA Stranded mRNA-Seq Kit (Kapa Biosystems, United Kingdom) and then sequenced on the Illumina NovaSeq 6000 platform. Raw reads were trimmed to remove the adapters and reads with a low sequencing quality score were eliminated using Cutadapt (v.3.5).[68] The retained high-quality reads were aligned to the Arabidopsis genome (TAIR10) using HISAT2 (v.2.2.1).[69] SAMtools (v.1.13) was used to obtain high-quality reads for mapping.[70] FeatureCounts (v.2.0.1) was used to calculate the read count for genes.[71] DESeq2 (v.1.32.0) was used to detect significant DEGs according to the following criteria: $p < 0.05$ and fold-change >1.5.[72] Track files in the bigwig format were obtained using bamCoverage in deepTools (v.3.5.1)[73] and then viewed using IGV (v.2.11.2).[74]

ChIP-seq analysis

DNA fragments obtained from PIF4-HA, H3K9ac, and H4K5ac ChIP were used in library construction and sequencing.[79] Cutadapt (v.3.5) was used to eliminate both adapters and low-quality sequencing reads from the raw reads.[68] The filtered reads were mapped to Arabidopsis thaliana genome (TAIR10) using Bowtie2 (v.2.4.5).[75] We then used SAMtools (v.1.13) to remove the PCR duplicates

and the low mapped quality reads.[70] MACS2 (v.2.2.7.1) was used to find peaks (p value <0.05).[76] MAnorm (v.1.3.0) was used to identify the differential peaks with the following thresholds: PIF4 ChIP-seq, p value <0.05, fold change >1.3; H3K9ac/H4K5ac ChIP-seq, p value <0.05, fold change >1.2.[77] Then, the peaks were annotated by using ChIPpeakAnno (v.3.28.1).[78] bamCoverage (v.3.5.1) was used to normalize the reads using RPKM, and computeMatrix (v.3.5.1) was used to calculate the enrichment signals.[73] Heatmaps were generated using the plotHeatmap (v.3.5.1).[73]

qRT-PCR analysis

Seedlings were grown on half-strength MS solid medium under continuous white light at 22°C for 6 days. The seedlings were then treated at 28°C (warm conditions) or 22°C (normal conditions) for 3 h. The plants used for the three biological replicates were from different plates but in the same growth chamber, and were harvested at the same time for RNA extraction. Total RNA was extracted from the seedlings using TRIzol reagent according to the manufacturer's instructions (Invitrogen, Carlsbad, CA, USA). The RNA was reverse transcribed using reverse transcriptase (Takara, Kusatsu, Shiga, Japan) according to the manufacturer's protocol. The qRT-PCR analysis was performed using specific primers (Table S1), with *ACTIN2* as the reference gene for normalizing expression data.

Yeast two-hybrid assay

The full-length *PIF4* and *MRG2* cDNA sequences were cloned into the pGADT7 (AD-PIF4) and pGBKT7 (BD-MRG2) vectors using specific primers (Table S1). The resulting recombinant plasmids were inserted into Y2HGold yeast cells according to the manufacturer's instructions (WeidiBio, Shanghai, China). Protein-protein interactions were screened on synthetic defined medium lacking tryptophan, leucine, and adenine (SD/−W/−L/−A).

GST pulldown assay

Full-length or truncated *PIF4* cDNA sequences (*PIF4-FL*, *PIF4-N1*, *PIF4-C1*, *PIF4-N2*, and *PIF4-C2*) were amplified by PCR using specific primers (Table S1) and then cloned into pGEX-6P-1. The pET28a-MRG2 recombinant plasmid was described previously.[46] The recombinant plasmids were inserted into Rosetta (DE3) competent cells. Proteins were purified using a kit according to the manufacturer's recommendations (GE Healthcare, Chicago, IL, USA). For the GST pulldown assay, GST-tagged fusion proteins were incubated with His-tagged fusion proteins for 2 h in GST binding buffer (1× PBS, 0.2% NP-40, and 1% BSA). Beads were washed three times using wash buffer (20 mM Tris-HCl, pH 8.0, 500 mM NaCl, and 0.5% NP-40). The proteins that were pulled down were examined in a western blot using an anti-His antibody (1:1,000 dilution) (GNI, GNI4110-HS).

Co-IP assay

Proteins were extracted from the *35S::PIF4-HA/35S::Flag-MRG2* transgenic plants grown under continuous white light at 22°C for 6 days. The Co-IP assay was performed as described previously.[46] The precipitated proteins were analyzed in a western blot using an anti-HA antibody (1:1,000 dilution) (Abcam, ab9110) and an anti-Flag antibody (1:2,000 dilution) (Sigma-Aldrich, F1804).

BiFC assay

Full-length or truncated *PIF4* cDNA sequences and the full-length *MRG2* cDNA sequence were amplified by PCR using specific primers (Table S1) and cloned into the pXY103 and pXY104 vectors. Different combinations of recombinant plasmids were inserted into *Nicotiana benthamiana* leaves via agroinfiltration. After 2 days, fluorescence was observed using the LSM 710 confocal laser scanning microscope (ZEISS, Germany).

ChIP-qPCR assay

Seedlings were grown at 22°C for 6 days and then treated at 28°C (warm conditions) or 22°C (normal conditions) for 6 h before they were harvested. The ChIP assays were performed as described previously, with a few modifications.[79] Briefly, seedlings were cross-linked for 15 min in fixative buffer (0.4 M sucrose, 10 mM Tris-HCl, pH 8.0, 1 mM EDTA, 1% formaldehyde, and 1 mM PMSF). The plant samples were ground to a powder in liquid nitrogen and then suspended in 25 mL lysis buffer [0.25 M sucrose, 15 mM PIPES, pH 6.8, 5 mM $MgCl_2$, 60 mM KCl, 15 mM NaCl, 1 mM $CaCl_2$, 0.9% Triton X-100, 1 mM PMSF, and a protease inhibitor cocktail tablet (14696200; Roche, Basel, Switzerland)]. After extracting the nuclei and sonicating, the supernatant was incubated overnight at 4°C in antibody buffer (50 mM HEPES, pH 7.5, 150 mM NaCl, 1 mM EDTA, 0.1% sodium deoxycholate, 1% Triton X-100, and a protease inhibitor cocktail tablet) containing one of the following antibodies: anti-H4K5ac (Sigma-Aldrich, 07–327), anti-H3K9ac (Abcam, ab10812), anti-H3K36ac (Active Motif, 39379), anti-H3K4me3 (Abcam, ab8580), anti-H3K36me3 (Abcam, ab9050), anti-HA (Abcam, ab9110), and anti-Myc (Abmart, M20002L). The samples were washed in the following solutions: low-salt buffer (150 mM NaCl, 20 mM Tris-HCl, pH 8.0, 0.2% SDS, 0.5% Triton X-100, and 2 mM EDTA), high-salt buffer (500 mM NaCl, 20 mM Tris-HCl, pH 8.0, 0.2% SDS, 0.5% Triton X-100, and 2 mM EDTA), lithium chloride wash buffer (0.25 M LiCl, 1% sodium deoxycholate, 10 mM Tris-HCl, pH 8.0, 1% NP-40, and 1 mM EDTA), and TE buffer (10 mM Tris-HCl, pH 8.0 and 1 mM EDTA). After the elution and the cross-linking reversal steps, the DNA was purified. The qRT-PCR analysis was performed using specific primers (Table S1), with *ACTIN2* serving as the control gene.

Competitive protein binding assay

The *phyB* cDNA sequences were amplified by PCR using primers listed in Table S1 and then cloned into pGEX-4T-1 and pCold-TF for the expression and purification of GST-phyB, and phyB proteins, individually. The methods for the protein purification and the *in vitro* competitive binding assay were the same as the methods used in the GST pulldown assay section described above. Notably, for the purification of phyB protein without tag, the tag was cleaved by Thrombin and dialyzed against buffer containing 20 mM Tris-HCl, pH 7.4 and 500 mM NaCl overnight at 20°C.[80] For the competitive binding assay involving the *35S::Flag-MRG2*/Col-0 plants, the samples were ground to a powder in liquid nitrogen and then suspended in lysis buffer (100 mM Tris-HCl, pH 7.5, 150 mM NaCl, 2 mM EDTA, pH 8.0, 10% glycerol, 2 mM DTT, 0.5% Triton X-100, 10 μM Phycocyanobilin (PCB), and a protease inhibitor cocktail tablet). The supernatant containing Flag-MRG2 proteins was incubated for 2–3 h with a prepared mixture comprising GST-phyB and His-PIF4 in dark, followed by exposure to red light for 10 min. Notably, phyB is the active Pfr form with the addition of PCB and treated with red light as previously described.[81] After washing four times with lysis buffer, the proteins were separated in SDS-PAGE gels and analyzed in a western blot using an anti-His antibody (GNI, GNI4110-HS), an anti-Flag antibody (Sigma-Aldrich, F1804), and an anti-phyB antibody (PHYTOAB, PHY1733).

Spilt luciferase assay

The full-length of cDNA encoding *PIF4* with HA epitope tag was fused with the DNA fragment encoding the N-terminal of the luciferase to create the *35S::nLUC-PIF4-HA* construct. Similarly, the *35S::cLUC-MRG2-Flag* construct was created by fusing the full-length cDNA encoding MRG2, along with a Flag epitope tag, with a DNA fragment encoding the C-terminal of luciferase. The *35S::cLUC-phyB* construct was generated by fusing the DNA fragment encoding phyB with the C-terminal of luciferase. To create the *35S::Flag-MRG2* and *35S::phyB-Myc* constructs, the full-length cDNA of *MRG2* and *phyB* were cloned into pCAMBIA1300. $phyB^{G111D}$*-Myc* was created by PCR using primers in Table S1. Different combinations of recombinant plasmids were inserted into *Nicotiana benthamiana* leaves via agroinfiltration. To measure luciferase activity, we injected luciferin into the positions where Agrobacterium was infiltrated. Subsequent luminescence imaging was performed using a CCD imaging system. To test the protein levels, a western blot assay was performed using the following antibodies: anti-HA (Abmart, M20003M), anti-phyB (PHYTOAB, PHY1733), anti-Flag (Abmart, M20008M), and anti-Myc (Abmart, M20002L).

Protein extraction and western blot assays

Seedlings were grown at 22°C for 6 days and then treated at 28°C (warm conditions) or 22°C (normal conditions) for 3, 6, and 12 h before they were harvested. The plant samples were ground to a powder in liquid nitrogen and then suspended in 200 μL extraction buffer (4% SDS and 50 mM Tris-HCl, pH 8.0). Samples were immediately boiled for 10 min, centrifuged at 14,000g for 10 min, separated in SDS-PAGE gels, and analyzed in a western blot using anti-PIF4 (Abiocode, R2534-4), anti-phyB (PHYTOAB, PHY1733), anti-H3 (Abcam, ab1791), and anti-ubiquitin (Beyotime, AF1705) antibodies.

QUANTIFICATION AND STATISTICAL ANALYSIS

The graphpad prism software *(Version 8.0.1*, http://www.graphpad-prism.cn/*)* was used to processed and analyzed the data by one-way ANOVA, followed by Fisher's LSD test ($p < 0.05$). Data were expressed as mean ± SD. The details about replicates and statistical methods for various experiments were provided in the figure legends. The p value of less than 0.05 was considered to be statistically significant (*$p < 0.05$ and ***$p < 0.001$).